Mol Neurobiol (2014) 49:1400–1421
DOI 10.1007/s12035-013-8617-1

Ginsenoside Re Rescues Methamphetamine-Induced Oxidative Damage, Mitochondrial Dysfunction, Microglial Activation, and Dopaminergic Degeneration by Inhibiting the Protein Kinase Cδ Gene

Eun-Joo Shin · Seung Woo Shin · Thuy-Ty Lan Nguyen · Dae Hun Park · Myung-Bok Wie · Choon-Gon Jang · Seung-Yeol Nah · Byung Wook Yang · Sung Kwon Ko · Toshitaka Nabeshima · Hyoung-Chun Kim

Received: 21 September 2013 / Accepted: 9 December 2013 / Published online: 16 January 2014

Abstract Ginsenoside Re, one of the main constituents of *Panax ginseng*, possesses novel antioxidant and anti-inflammatory properties. However, the pharmacological mechanism of ginsenoside Re in dopaminergic degeneration remains elusive. We suggested that protein kinase C (PKC) δ mediates methamphetamine (MA)-induced dopaminergic toxicity. Treatment with ginsenoside Re significantly attenuated methamphetamine-induced dopaminergic degeneration in vivo by inhibiting impaired enzymatic antioxidant systems, mitochondrial oxidative stress, mitochondrial translocation of protein kinase Cδ, mitochondrial dysfunction, pro-inflammatory microglial activation, and apoptosis. These protective effects were comparable to those observed with genetic inhibition of PKCδ in PKCδ knockout (−/−) mice and with PKCδ antisense oligonucleotides, and ginsenoside Re did not provide any additional protective effects in the presence of PKCδ inhibition. Our results suggest that PKCδ is a critical target for ginsenoside Re-mediated protective activity in response to dopaminergic degeneration induced by MA.

Keywords Ginsenoside Re · Methamphetamine · Protein kinase C δ · Dopamine · Mitochondria · Apoptosis · Oxidative damage

Electronic supplementary material The online version of this article (doi:10.1007/s12035-013-8617-1) contains supplementary material, which is available to authorized users.

E.-J. Shin · S. W. Shin · T.-T. L. Nguyen · D. H. Park · H.-C. Kim (✉)
Neuropsychopharmacology and Toxicology Program, College of Pharmacy, Kangwon National University, Chunchon 200-701, Republic of Korea
e-mail: kimhc@kangwon.ac.kr

D. H. Park
Department of Oriental Medicine Materials, Dongshin University, Naju 520-714, Republic of Korea

M.-B. Wie
School of Veterinary Medicine, Kangwon National University, Chunchon 200-701, Republic of Korea

C.-G. Jang
Department of Pharmacology, School of Pharmacy, Sungkyunkwan University, Suwon 440-746, Republic of Korea

S.-Y. Nah
Ginsentology Research Laboratory and Department of Physiology, College of Veterinary Medicine and Bio/Molecular Informatics Center, Konkuk University, Seoul 143-701, Republic of Korea

B. W. Yang
Department of Systems Biotechnology, Chung-Ang University, Anseong 456-756, Republic of Korea

S. K. Ko (✉)
Department of Oriental Medical Food & Nutrition, Semyung University, Jecheon, Choongbuk 390-711, Republic of Korea
e-mail: skko@semyung.ac.kr

T. Nabeshima
Department of Regional Pharmaceutical Care & Science, Graduate School of Pharmaceutical Sciences, Meijo University, Nagoya 468-8503, Japan

Introduction

High doses of methamphetamine (MA) can lead to dopaminergic neurotoxicity. Previous reports have raised the possibility that MA abuse increases the risk for Parkinson's disease (PD) later in life [1–3]. Postmortem studies have demonstrated that reductions in dopamine (DA) level, tyrosine hydroxylase (TH) expression, and dopamine transporter (DAT) binding are observed in the striatum of MA abusers [4] and that these changes parallel, at least in part, neurochemical changes in patients with PD [5, 6]. Earlier reports suggested that MA-induced dopaminergic toxicity is, at least in part, similar to 1-methyl-4-phenyl-1,2,3,6-tetrahydropyridine (MPTP)-induced toxicity in mice [7, 8].

Ginseng has an important position in traditional medicine in far eastern Asian countries [9]. Although the pharmacological mechanism of ginseng remains elusive, the therapeutic effects of ginseng have been attributed to its active components, called ginsenosides, which are sugar conjugates of dihydroxyl or trihydroxyl dammarane triterpenes. Ginsenosides are normally fractioned into two groups based on the type of aglycone, namely the protopanaxadiol (e.g., ginsenosides Re and Rg1) and protopanaxatriol (e.g., ginsenosides Rb1 and Rc) groups.

Ginsenoside Re ($C_{53}H_{90}O_{22}$) (Fig. 1a) is a main ginsenoside and an important ingredient in ginseng leaf, berry, and root [10–13]. It exhibits different pharmacological activities via multiple mechanisms both in vivo and in vitro [11, 14–18]. Xu et al. [18] demonstrated that ginsenoside Re attenuates MPTP-induced nigral apoptosis in mice. Kim et al. [17] demonstrated that it prevents mitochondrial complex IV deficits in the PINK 1 null dopaminergic neuronal cell line via restoration of nitric oxide (NO) signaling. However, the precise pharmacological mechanism mediated by ginsenoside Re in response to dopaminergic degeneration in vivo remains to be further characterized.

Protein kinase C (PKC) is a family of multiple isozymes that play a crucial role in the regulation of cellular proliferation and differentiation [19]. The PKC family is divided into several subfamilies, and individual members have a tissue-specific distribution and mode of activation, as well as kinetics and substrate specificities, suggesting that individual or subgroups of PKC isozymes play discrete roles within cells [20]. However, different and conflicting effects of PKCs on apoptosis in various model systems have made it difficult to define their role in toxicity [21]. Earlier reports suggested that PKCδ is a functional tyrosine phosphorylation modulator of tyrosine hydroxylase that plays a key role in apoptotic cell death of dopaminergic neurons [22–24].

We have recently suggested that PKCδ mediates MA-induced dopaminergic neurodegeneration by potentiating oxidative damage and inhibiting TH phosphorylation [25, 26]. We have also demonstrated that ginsenosides attenuate MA-induced psychotoxicity associated with enhanced AP-1 DNA binding activity and proenkephalin expression by modulating the adenosine A_{2A} receptor [27]. However, little is known about the effect of ginsenosides on PKCδ upregulation induced by MA. We suggest here that ginsenoside Re attenuates MA-induced dopaminergic degeneration in vivo mainly by inhibiting impaired enzymatic antioxidant system, mitochondrial oxidative stress, mitochondrial translocation of PKCδ, mitochondrial dysfunction, pro-inflammatory microglial activation, and apoptosis.

Materials and Methods

Animal and Drug Treatment

All mice were treated in accordance with the NIH Guide for the Humane Care and Use of Laboratory Animals. They were maintained on a 12/12-h light/dark cycle and fed ad libitum. They were adapted to these conditions for 2 weeks before the experiment. A breeding pair of PKCδ (+/−) mice, originally bred into a C57BL/6 background, was a gift from Dr. K.I. Nakayama (Department of Molecular Genetics, Medical Institute of Bioregulation, Kyushu University, Fukuoka, Japan) [28]. These mice were subsequently maintained and bred into the C57BL/6 background for three to six generations in an SPF mice facility before use with PKCδ (+/+) mice from the same litter in our experiments. The details of the genotyping procedure are provided in the supplementary information section.

High-performance liquid chromatography grade ginsenoside Re with greater than 99 % purity was provided by Dr. Sung Kwon Ko [12, 13] (Fig. 1a). Mice received four doses of MA (8 mg/kg, i.p.) or saline at 2-h intervals. Administration of ginsenoside Re (10 or 20 mg/kg, p.o., twice a day) was started at 5 days before MA injection and then continued throughout the experimental period. On the day of MA injection, ginsenoside Re was administered at 2 h before the first MA injection and 4 h after the final MA injection. Behavioral assessments were conducted at 2 h, 6 h, 1 day, 3 days, and 14 days after the final MA injection, and then, mice were sacrificed for neurochemical and histochemical analyses. Additional mice were sacrificed for evaluating mitochondrial function or immunocytochemistry at 6 h or 3 days after the final MA injection, respectively. The experimental schedule was shown in Fig. 1b.

For evaluating the effect of ginsenoside Re on the MA-induced apoptosis, we employed 10-week-old male ICR mice (Taconic Farms, Inc., Samtako Bio Korea, O-San, South Korea). Our previous report [26] indicated that PKCδ (+/+) mice do not show MA-induced terminal deoxynucleotidyl

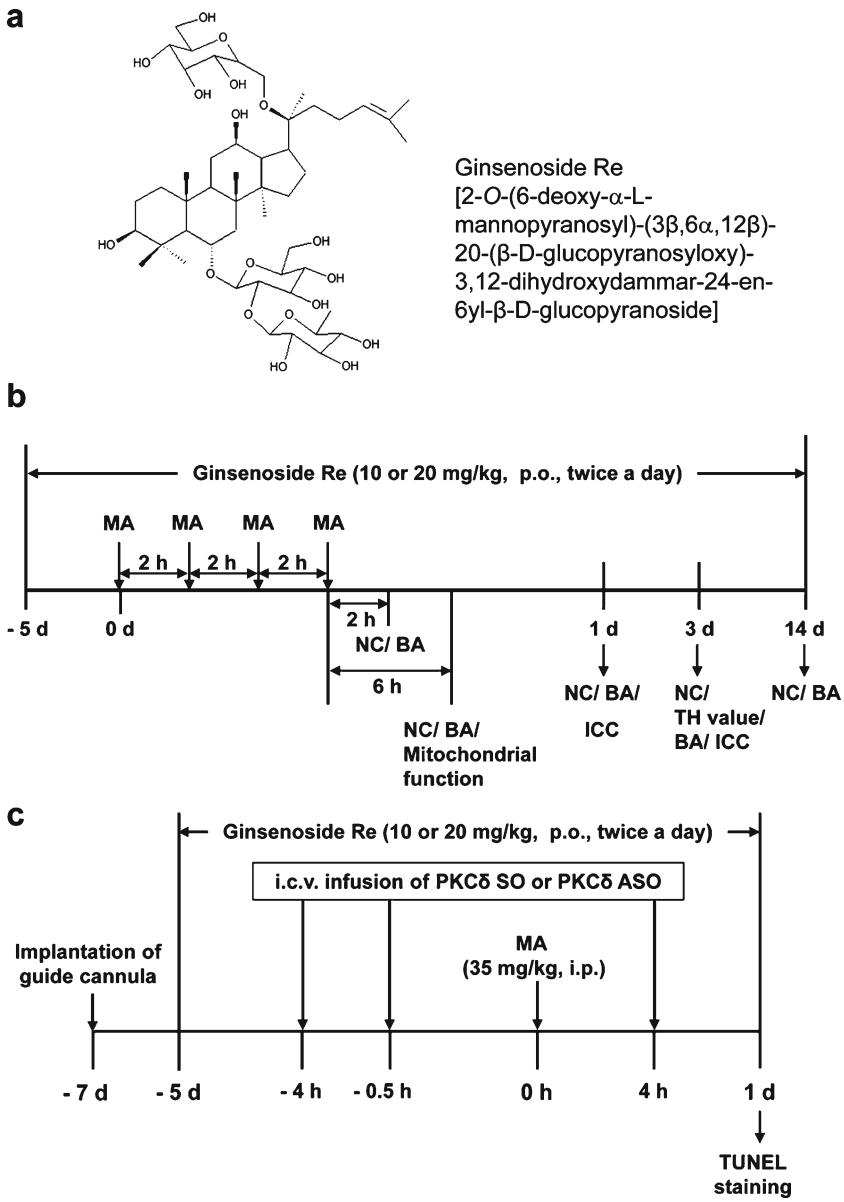

Fig. 1 Experimental design for evaluating the effects of ginsenoside Re on MA-induced dopaminergic neurodegeneration. **a** Chemical structure of ginsenoside Re. **b** Experimental design using PKCδ (+/+) and PKCδ (−/−) mice. See text for details. *BA* behavioral assessments, *NC* neurochemical analyses, *TH value* TH immunoreactivity (by immunostaining), TH protein expression, and TH activity, *ICC* immunocytochemistry. **c** Experimental design for TUNEL staining using Taconic ICR mice. *PKCδ SO* protein kinase C sense oligonucleotide (SO), *PKCδ ASO* protein kinase C antisense oligonucleotide (ASO)

transferase dUTP nick end labeling (TUNEL)-positive cells in the striatum, but Taconic ICR mice do [26, 29, 30]. Mice received ginsenoside Re (20 mg/kg, p.o., twice per day) for 5 days before MA injection with an additional treatment (20 mg/kg, p.o., twice per day) on the day after MA injection.

To examine whether PKCδ can be a pharmacological target of ginsenoside Re, PKCδ antisense oligonucleotides (PKCδ ASO; 5′-GAAGGCGATGCGCAGGAA; Bioneer Corp., Daejeon, Republic of Korea) [31] or control PKCδ sense oligonucleotides (PKCδ SO; 5′-AGGAACGGCGCCATGG TGGG; Bioneer) [31] were microinfused into the lateral ventricle at a dose of 2.5 μg/μL at 4 and 0.5 h before and at 4 h after MA injection. Mice were sacrificed 1 day after MA injection [26]. The experimental schedules are shown in Fig. 1c. Additional details on the guide cannula implantation and microinfusion with PKCδ ASO or control PKCδ SO are described in the Supplementary Information.

Preparation of Cytosolic and Mitochondrial Fractions

The cytosolic and mitochondrial fractions were prepared as described previously for Western blot analysis and the neurochemical assay [32]. Mitochondria were isolated as described previously [33] with minor modifications [34] for measurements of mitochondrial membrane potential and intramitochondrial Ca^{2+} level in the striatum of mice. The details of the procedure are provided in the Supplementary Information.

Tissue Preparation for Enzyme Activity Assays

Striatal tissues were homogenized in 50 mM potassium phosphate buffer (pH 7.0) and centrifuged at 13,000×*g* for 20 min. The resulting supernatant was used to measure the activities of glutathione peroxidase (GPx), glutathione *S*-transferase, and catalase. Additional striatal tissues were homogenized in 50 mM potassium phosphate buffer (pH 7.8) and centrifuged at 13,000×*g* for 20 min. The resulting supernatant was used to measure the activities of superoxide dismutase (SOD) and glutathione reductase. For measurement of cytosolic and mitochondrial GPx activity, subcellular fractionation was performed as described in the Supplementary Information.

Determination of SOD Activity

SOD activity was determined on the basis of inhibition of superoxide-dependent reactions as described previously [7, 35]. The reaction mixture contained 70 mM potassium phosphate buffer (pH 7.8), 30 μM cytochrome c, 150 μM xanthine, and tissue extract in phosphate buffer diluted tenfold with PBS in a final volume of 3 mL. The reaction was initiated by adding 10 μL of 50 units xanthine oxidase, and the change in absorbance at 550 nm was recorded. One unit of SOD was defined as the quantity required inhibiting the rate of cytochrome c reduction by 50 %. For estimating total SOD, 10 μM potassium cyanide (KCN) was added to the medium to inhibit cytochrome oxidase activity. For estimating mitochondrial Mn-SOD activity, 1 mM KCN was added to the incubation mixture to inhibit Cu, Zn-SOD activity. The activity of cytosolic Cu, Zn-SOD was calculated by subtraction of the mitochondrial Mn-SOD activity from the total SOD activity.

Determination of Catalase

Catalase activity was determined by the rate of hydrogen peroxide absorbance decrease at 240 nm [36]. The reaction mixture contained 50 mM potassium phosphate buffer (pH 7.0) and an aliquot of the sample. The reaction started with adding hydrogen peroxide (final concentration of 10 mM), and absorbance was monitored at 25 °C for 5 min. Catalase from bovine liver (Sigma-Aldrich, St. Louis, MO, USA) was used as a standard.

Determination of Glutathione Peroxidase

GPx activity was analyzed by a spectrophotometric assay described by Lawrence and Burk [37], using 2.0 mM reduced glutathione and 0.25 mM cumene hydroperoxide as substrates. The reaction rate at 340 nm was determined using the NADPH extinction coefficient (6.22 mM^{-1} cm^{-1}). GPx activity was expressed as nanomole NADPH oxidized per minute per milligram protein at 25 °C. Protein was measured using the BCA protein assay reagent and bovine serum albumin was used as a standard.

Reverse Transcription and Polymerase Chain Reaction

Total RNA from the striatum was isolated using an RNeasy Mini Kit (Qiagen). Reverse transcription was performed by incubation for 1 h at 37 °C in reaction mixtures containing AMV transcriptase and random oligonucleotide primers. PCR amplification was performed for 35 cycles of denaturation at 94 °C for 1 min, annealing at 60 °C for 2 min, and extension at 72 °C for 1 min. Primer sequences [38] for PCR amplification are listed in Supplementary Table 1. PCR products were separated on 2 % agarose gels containing ethidium bromide. Quantitative analysis of RNA was performed using PhotoCaptMw computer software (Vilber Lourmat, Marne-la-Vallée, France).

Immunocytochemistry

Immunocytochemistry and quantitative analyses were performed as described previously [38]. Mice were perfused transcardially with 50 mL of ice-cold PBS (10 mL/10 g body weight) followed by 4 % paraformaldehyde (20 mL/10 g body weight). Brains were removed and stored in 4 % paraformaldehyde overnight. Sections were subjected to immunostaining with primary antibody against glial fibrillary acidic protein (GFAP) [1:250; Chemicon (EMD Millipore), Temecula, CA, USA], Iba-1 (1:400; Abcam, Cambridge, UK), or TH [1:500; Chemicon (EMD Millipore)]. ImageJ version 1.44 software (National Institutes of Health, Bethesda, MD, USA) was employed to measure the immunoreactivities of TH, GFAP, and Iba-1 in the striatum. The details on immunocytochemistry and quantitative analysis are described in the Supplementary Information section.

Stereological Analyses

The total number of immunolabeled TH, GFAP, or Iba-1 cells in the substantia nigra (SN) pars compacta was estimated using the stereological analysis method as described previously [38, 39]. The details of the procedure are provided in the Supplementary Information section.

Western Blot Analysis

PKCδ and cleaved PKCδ were examined in the mitochondrial and cytosolic fractions prepared from striatal tissues. For Western blot analysis of TH, striatal tissues were lysed in buffer containing 200 mM Tris–HCl (pH 6.8), 1 % SDS, 5 mM ethylene glycol-bis(2-aminoethyl ether)-*N*,*N*,*N*′,*N*′-tetraacetic acid, 5 mM ethylenediaminetetraacetic acid, 10 % glycerol, and 1× protease inhibitor cocktail (Sigma-Aldrich,

St. Louis, MO, USA). Lysate was centrifuged at 12,000×*g* for 30 min, and the supernatant was used for Western blot analysis as described previously [40, 41]. Additional details on the procedure and antibody are provided in the Supplementary Information.

Determination of 4-Hydroxynonenal and Protein Carbonyl

The amount of lipid peroxidation was determined by measuring the level of 4-hydroxynonenal (HNE) using the OxiSelect™ HNE adduct ELISA kit (Cell Biolabs, Inc., San Diego, CA, USA) according to the manufacturer's manual. Briefly, HNE adducts in the cytosolic and mitochondrial fractions obtained from striatal tissues were adsorbed in a 96-well protein-binding plate. Adsorbed HNE adducts were detected by HNE antibody. HNE-BSA was used as the standard.

The extent of protein oxidation was assessed by measuring the content of protein carbonyl groups, which was determined spectrophotometrically using the 2,4-dinitrophenylhydrazine-labeling procedure [27] as described by Oliver et al. [42]. Additional details on the determination of HNE and protein carbonyl are provided in the Supplementary Information.

TUNEL Staining

TUNEL staining was performed using the FragEL DNA Fragmentation Detection kit (QIA33; Calbiochem, La Jolla, CA, USA) for in vivo striatal sections according to the manufacturer's protocol [26]. Details are described in the Supplementary Information.

Mitochondrial Transmembrane Potential and Intramitochondrial Ca^{2+} Levels in the Striatum of Mice

Mitochondrial transmembrane potential was measured as described previously [34, 43, 44] using the dye 5,5′,6,6′-tetrachloro-1,1′,3,3′-tetraethylbenzimidazolycarbocyanine iodide (JC-1; Molecular Probes Inc., Eugene, OR, USA), which exists as a green fluorescent monomer at low membrane potential, but reversibly forms red fluorescent "J-aggregates" at polarized mitochondrial potentials. Intramitochondrial Ca^{2+} levels were measured as described previously [34, 45, 46], using the Ca^{2+} indicator rhod-2-AM (Molecular Probes Inc.). The details of the procedure are provided in the Supplementary Information.

Measurement of Dopamine Level

Mice were sacrificed by cervical dislocation and the brains were removed. The striatum was dissected, immediately frozen on dry ice, and stored at −70 °C before assays were performed. Tissues were weighed, ultrasonicated in 10 % perchloric acid, and centrifuged at 20,000×*g* for 10 min. The dopamine level was determined by high-performance liquid chromatography (HPLC) coupled with an electrochemical detector as described previously [26]. Additional details on the HPLC conditions are provided in the Supplementary Information.

Measurement of TH Activity

TH activity was measured according to the method of Nagatsu et al. [47] with slight modification [26]. Briefly, the striatum was homogenized in ice-cold 0.05 M sodium acetate buffer (pH 6.0), and the homogenate was centrifuged (3,000×*g*, 10 min). The supernatant was added to reaction mixture including L-tyrosine, and then, reactions were incubated for 10 min at 37 °C. The DOPA formation was analyzed by HPLC apparatus equipped with electrochemical detector (ECD-300, Eicom, Kyoto, Japan). TH activity was expressed as picomole of DOPA formation per milligram wet tissue per minute. Additional details on reaction procedure and HPLC conditions are provided in the Supplementary Information section.

Locomotor Activity

Locomotor activity was measured for 30 min using an automated video-tracking system (Noldus Information Technology, Wagenin, The Netherlands). Four test boxes (40×40×30 cm high) were operated simultaneously by an IBM computer. Each mouse was placed in each test box and then adapted for 5 min before starting the experiment. A printout for each session showed the pattern of the ambulatory movements of the test box. The distance traveled in centimeter by the animals in horizontal locomotor activity was analyzed. Data were collected and analyzed between 09:00 and 17:00 hours [25].

Rotarod Test

The apparatus (Ugo Basile model 7650, Comerio, VA, Italy) consisted of a base platform and a rotating rod with a non-slippery surface. The rod was placed at a height of 15 cm from the base. The rod, 30 cm in length, was divided into five equal sections by six opaque disks (so that the subjects cannot be distracted by one another). To assess motor performance, the mice first trained on the apparatus for 2 min at a constant rate of 4 rpm. The test was performed 30 min after training and an accelerating paradigm was applied, starting from a rate of 4 rpm to a maximum speed of 40 rpm, then the rotation speed was kept constant at 40 rpm for a maximum of 300 s. The duration for which the animal could maintain balance on the rotating drum was measured as the latency to fall, with a maximal cutoff time of 300 s [25].

Statistical Analyses

Data were analyzed using IBM SPSS ver. 21.0 (IBM, Chicago, IL, USA). Three-way analysis of variance (ANOVA) (PKCδ gene knockout or PKCδ ASO × ginsenoside Re × MA) or four-way ANOVA (PKCδ gene knockout or PKCδ ASO × ginsenoside Re × MA × time points) was employed for the statistical analyses. A repeated-measures ANOVA (between-subjects factors: PKCδ gene knockout × ginsenoside Re × MA; within-subjects factor: time) was conducted for the behavioral measurements. Post hoc multiple pairwise comparisons with Bonferroni's correction were then conducted. P values<0.05 were considered to be significant.

Results

Protective Effects of Ginsenoside Re on MA-Induced Changes in SOD, Catalase, and GPx Activities Mediated by PKCδ

The enzymes involved in cellular defense against oxidative damage have been repeatedly proposed to be SOD, catalase, and peroxidases such as GPx. It seems reasonable to assume that these enzymes work in concert, as SOD catalyzes $O_2^{\cdot-}$ (superoxide anion) dismutation to produce H_2O_2, whereas catalase or GPx removes it. However, it is also apparent that the presence of catalase is restricted in most eukaryotic cells to isolated compartments such as peroxisomes, whereas SOD and peroxidases, which is essentially GPx in animal cells, are present in the cytoplasmic and mitochondrial fractions [48–50]. In the present study, we examined whether ginsenoside Re or genetic inhibition of PKCδ modulated SOD, catalase, and GPx activities in the presence of MA.

Figure 2 shows striatal changes in the enzymatic activities of SOD, catalase, and GPx in PKCδ (+/+) and PKCδ (−/−)-mice. In the absence of MA, there was no significant difference between PKCδ (+/+) and PKCδ (−/−) mice in terms of SOD, catalase, or GPx activity. ANOVA indicated significant effects of PKCδ gene knockout (SOD: $F_{1,\ 200}$= 5.77, P=0.0172; catalase: $F_{1,\ 200}$=10.27, P=0.00157; GPx: $F_{1,\ 200}$=5.90, P=0.0160), MA (SOD: $F_{1,\ 200}$=42.04, P=6.86× 10^{-10}; catalase: $F_{1,\ 200}$=65.48, P=1.56×10^{-13}; GPx: $F_{1,\ 200}$= 19.17, P=2.03×10^{-5}), ginsenoside Re (GPx: $F_{2,\ 200}$=6.24, P=0.00236), and time points (SOD: $F_{4,\ 200}$=4.64, P=0.00133; catalase: $F_{4,\ 200}$=6.33, P=8.18×10^{-5}). We further observed significant interactions between PKCδ gene knockout and MA (SOD: $F_{1,\ 200}$=4.59, P=0.0335; catalase: $F_{1,\ 200}$= 5.09, P=0.0252; GPx: $F_{1,\ 200}$=10.77, P=0.00122), PKCδ gene knockout and ginsenoside Re (GPx: $F_{2,\ 200}$=3.18, P=0.0435), ginsenoside Re and MA (SOD: $F_{1,\ 200}$= 4.37, P=0.0378; catalase: $F_{1,\ 200}$=8.05, P=0.00502; GPx: $F_{1,\ 200}$=5.84, P=0.0166), and MA and time points (catalase: $F_{4,\ 200}$=3.07, P=0.0176). A post hoc test revealed that treatment with MA resulted in significant increases in SOD activity [at 2 h, P=0.0421; at 6 h, P=1.65×10^{-5}; at 1 day, P=5.94×10^{-4}; at 3 days, P=0.0164 vs. corresponding saline (Sal) + Sal] in the PKCδ (+/+) mice. The MA-induced increase in SOD activity appeared to be most pronounced 6 h after the last MA administration. Ginsenoside Re (at 6 h, P=0.0487 vs. corresponding Sal + MA) or PKCδ gene knockout (at 6 h, P=0.0120 vs. corresponding Sal + MA) significantly attenuated this increase in SOD activity in PKCδ (+/+) mice. Similarly, MA treatment significantly increased catalase activity (at 2 h, P=0.0394; at 6 h, P=4.84×10^{-4}; at 1 day, P=3.09×10^{-7}; at 3 daya, P=0.00178 vs. corresponding Sal + Sal) in the PKCδ (+/+) mice. The MA-induced increase in catalase activity was most pronounced 1 day after the last MA administration. PKCδ gene knockout (at 1 day, P=0.0184 vs. corresponding saline + MA) or ginsenoside Re (at 1 day, P=0.0314 vs. corresponding Sal+MA) significantly attenuated increased catalase activity in the PKCδ (+/+) mice. In contrast, MA-induced significant decreases in GPx activity (at 6 h, P=3.19×10^{-5}; at 1 day, P=6.74×10^{-4}; at 3 days, P=0.00670 vs. corresponding Sal + Sal) in PKCδ (+/+) mice. The MA-induced decrease in GPx activity was most pronounced 6 h after the last MA administration. Ginsenoside Re (at 6 h, P=0.00391; at 1 day, P=0.0249; at 3 day, P=0.0190 vs. corresponding Sal + MA) or PKCδ gene knockout (at 6 h, P=0.00305; at 1 day, P=0.00519; at 3 day, P=0.00275 vs. corresponding saline + MA) significantly attenuated decreased GPx activity induced by MA in the PKCδ (+/+) mice. Ginsenoside Re treatment did not significantly affect attenuations mediated by PKCδ gene knockout. In addition, glutathione reductase and glutathione *S*-transferase activities were also decreased after MA treatment in the PKCδ (+/+) mice (Supplementary Fig. 1). However, effects of ginsenoside Re or PKCδ gene knockout on these activities were less pronounced than those on GPx activity induced by MA.

Protective Effects of Ginsenoside Re on MA-Induced Oxidative Damage Mediated by PKCδ Indicates that the Mitochondrial Fraction Is More Susceptible than the Cytosolic Fraction to Ginsenoside Re

We reported recently that activation of PKCδ is a key mediator of oxidative stress and dopaminergic damage induced by MA [26]. Although MA-induced oxidative stress is well recognized, the mechanism underlying MA-induced mitochondrial oxidative damage remains elusive. In the present study, we performed time-course assessments in response to MA-induced oxidative damage. We examined whether ginsenoside Re attenuates protein oxidation (i.e., protein carbonyl) and lipid peroxidation [i.e., HNE] induced by MA.

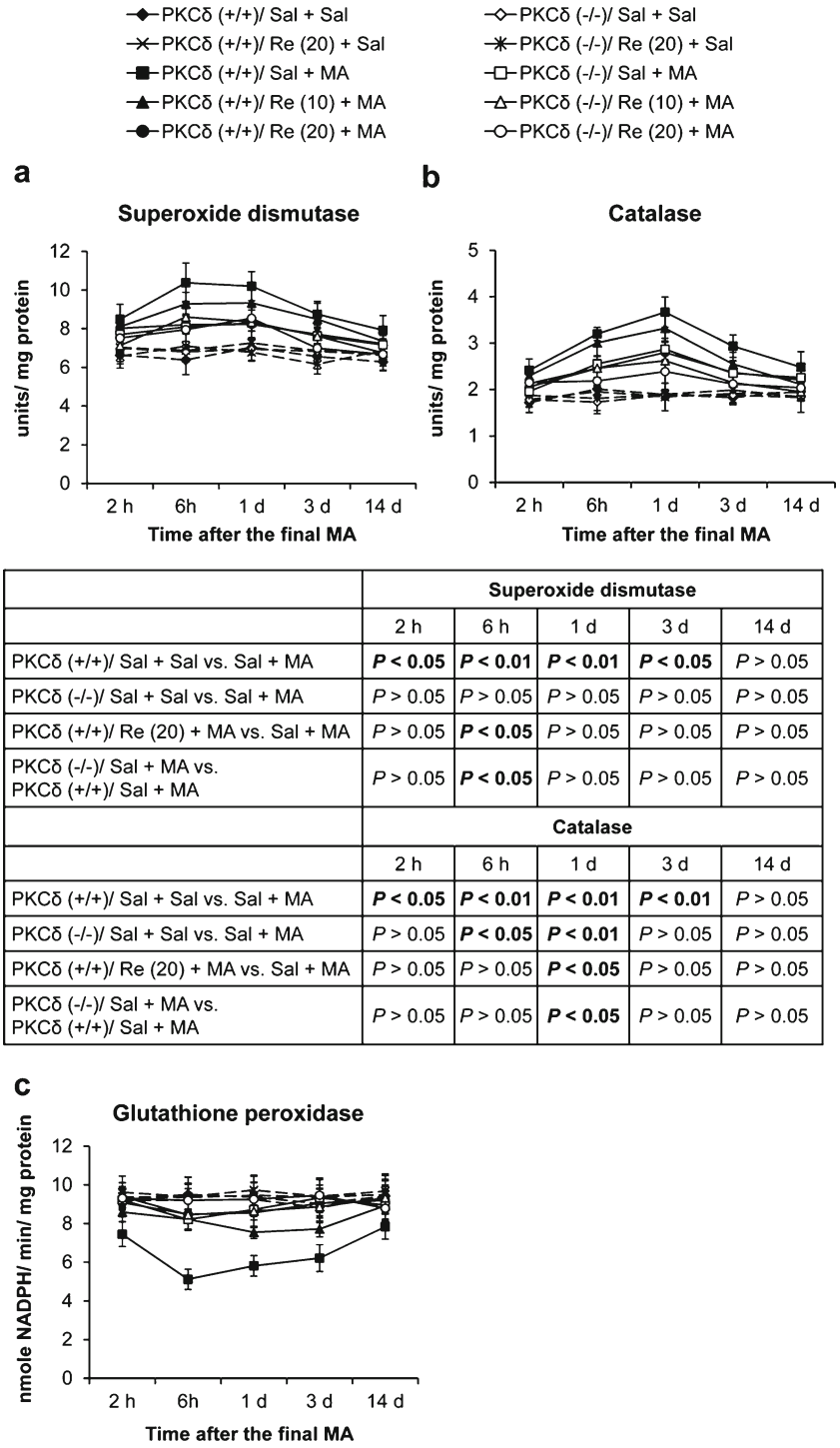

Fig. 2 Effect of ginsenoside Re on changes in antioxidant enzymatic activity induced by methamphetamine (*MA*) in the striatum of PKCδ (+/+) and PKCδ (−/−) mice. **a** Effect on activity of superoxide dismutase induced by MA. **b** Effect on activity of catalase induced by MA. **c** Effect on activity of glutathione peroxidase induced by MA. *Sal* saline, *Re (10)* ginsenoside Re (10 mg/kg, p.o.), *Re (20)* ginsenoside Re (20 mg/kg, p.o.). Each value is the mean ± S.E.M. of five animals. *P* values were shown below the figure (four-way ANOVA followed by multiple pairwise comparisons with Bonferroni's correction)

	Superoxide dismutase				
	2 h	6 h	1 d	3 d	14 d
PKCδ (+/+)/ Sal + Sal vs. Sal + MA	***P* < 0.05**	***P* < 0.01**	***P* < 0.01**	***P* < 0.05**	*P* > 0.05
PKCδ (-/-)/ Sal + Sal vs. Sal + MA	*P* > 0.05	*P* > 0.05	*P* > 0.05	*P* > 0.05	*P* > 0.05
PKCδ (+/+)/ Re (20) + MA vs. Sal + MA	*P* > 0.05	***P* < 0.05**	*P* > 0.05	*P* > 0.05	*P* > 0.05
PKCδ (-/-)/ Sal + MA vs. PKCδ (+/+)/ Sal + MA	*P* > 0.05	***P* < 0.05**	*P* > 0.05	*P* > 0.05	*P* > 0.05
	Catalase				
	2 h	6 h	1 d	3 d	14 d
PKCδ (+/+)/ Sal + Sal vs. Sal + MA	***P* < 0.05**	***P* < 0.01**	***P* < 0.01**	***P* < 0.01**	*P* > 0.05
PKCδ (-/-)/ Sal + Sal vs. Sal + MA	*P* > 0.05	***P* < 0.05**	***P* < 0.01**	*P* > 0.05	*P* > 0.05
PKCδ (+/+)/ Re (20) + MA vs. Sal + MA	*P* > 0.05	*P* > 0.05	***P* < 0.05**	*P* > 0.05	*P* > 0.05
PKCδ (-/-)/ Sal + MA vs. PKCδ (+/+)/ Sal + MA	*P* > 0.05	*P* > 0.05	***P* < 0.05**	*P* > 0.05	*P* > 0.05

	Glutathione peroxidase				
	2 h	6 h	1 d	3 d	14 d
PKCδ (+/+)/ Sal + Sal vs. Sal + MA	*P* > 0.05	***P* < 0.01**	***P* < 0.01**	***P* < 0.01**	*P* > 0.05
PKCδ (-/-)/ Sal + Sal vs. Sal + MA	*P* > 0.05	*P* > 0.05	*P* > 0.05	*P* > 0.05	*P* > 0.05
PKCδ (+/+)/ Re (20) + MA vs. Sal + MA	*P* > 0.05	***P* < 0.01**	***P* < 0.05**	***P* < 0.05**	*P* > 0.05
PKCδ (-/-)/ Sal + MA vs. PKCδ (+/+)/ Sal + MA	*P* > 0.05	***P* < 0.01**	***P* < 0.01**	***P* < 0.01**	*P* > 0.05

ANOVA indicated significant effects of PKCδ gene knockout (cytosolic protein carbonyl: $F_{1,\ 250}=23.83$, $P=1.87\times10^{-6}$; mitochondrial protein carbonyl: $F_{1,\ 250}=20.75$, $P=8.17\times10^{-6}$; cytosolic HNE: $F_{1,\ 250}=19.04$, $P=1.87\times10^{-5}$; mitochondrial HNE: $F_{1,\ 250}=31.94$, $P=4.33\times10^{-8}$), MA (cytosolic protein carbonyl: $F_{1,\ 250}=315.07$, $P=3.61\times10^{-46}$; mitochondrial protein carbonyl: $F_{1,\ 250}=140.85$, $P=4.59\times10^{-26}$; cytosolic HNE: $F_{1,\ 250}=286.77$, $P=2.27\times10^{-43}$; mitochondrial HNE: $F_{1,\ 250}=392.78$, $P=3.49\times10^{-53}$), ginsenoside Re (cytosolic protein carbonyl: $F_{2,\ 250}=4.41$, $P=0.013$; cytosolic HNE: $F_{2,\ 250}=8.07$, $P=4.03\times10^{-4}$; mitochondrial HNE: $F_{2,\ 250}=11.22$, $P=2.163\times10^{-5}$), and time points (cytosolic protein carbonyl: $F_{4,\ 250}=47.25$, $P=1.49\times10^{-29}$; mitochondrial protein carbonyl: $F_{4,\ 250}=35.41$, $P=1.99\times10^{-23}$; cytosolic HNE: $F_{4,\ 250}=57.29$, $P=2.92\times10^{-34}$; mitochondrial HNE: $F_{4,\ 250}=57.62$, $P=2.07\times10^{-34}$), and significant interactions between PKCδ gene knockout and MA (cytosolic protein carbonyl: $F_{1,\ 250}=21.66$, $P=5.29\times10^{-6}$; mitochondrial protein carbonyl: $F_{1,\ 250}=24.33$, $P=1.48\times10^{-6}$; cytosolic HNE: $F_{1,\ 250}=13.75$, $P=2.57\times10^{-4}$; mitochondrial HNE: $F_{1,\ 250}=42.35$, $P=4.14\times10^{-10}$), PKCδ gene knockout and ginsenoside Re (mitochondrial protein carbonyl: $F_{2,\ 250}=7.77$, $P=0.000532$; cytosolic HNE: $F_{2,\ 250}=4.38$, $P=0.0134$; mitochondrial HNE: $F_{2,\ 250}=8.03$, $P=4.18\times10^{-4}$), PKCδ gene knockout and time points (mitochondrial protein carbonyl: $F_{4,\ 250}=9.19$, $P=6.09\times10^{-7}$; cytosolic HNE: $F_{4,\ 250}=2.67$, $P=0.0331$; mitochondrial HNE: $F_{4,\ 250}=10.92$, $P=3.53\times10^{-8}$), ginsenoside Re and MA (cytosolic protein carbonyl: $F_{1,\ 250}=20.73$, $P=8.26\times10^{-6}$; mitochondrial protein carbonyl: $F_{1,\ 250}=17.26$, $P=4.48\times10^{-5}$; cytosolic HNE: $F_{1,\ 250}=18.08$, $P=2.99\times10^{-5}$; mitochondrial HNE: $F_{1,\ 250}=23.57$, $P=2.12\times10^{-6}$), ginsenoside Re and time points (mitochondrial protein carbonyl: $F_{8,\ 250}=2.32$, $P=0.0201$; mitochondrial HNE: $F_{8,\ 250}=2.19$, $P=0.0288$), MA and time points (cytosolic protein carbonyl: $F_{4,\ 250}=30.06$, $P=1.99\times10^{-20}$; mitochondrial protein carbonyl: $F_{4,\ 250}=26.51$, $P=2.46\times10^{-18}$; cytosolic HNE: $F_{4,\ 250}=23.70$, $P=1.25\times10^{-16}$; mitochondrial HNE: $F_{4,\ 250}=37.41$, $P=1.64\times10^{-24}$), PKCδ gene knockout and ginsenoside Re and MA (mitochondrial protein carbonyl: $F_{1,\ 250}=14.83$, $P=1.49\times10^{-4}$; cytosolic HNE: $F_{1,\ 250}=5.81$, $P=0.0166$; mitochondrial HNE: $F_{1,\ 250}=11.32$, $P=8.87\times10^{-4}$), PKCδ gene knockout and ginsenoside Re and time points (mitochondrial protein carbonyl: $F_{8,\ 250}=2.25$, $P=0.0262$), PKCδ gene knockout and MA and time points (mitochondrial protein carbonyl: $F_{4,\ 250}=5.72$, $P=0.000203$; mitochondrial HNE: $F_{4,\ 250}=4.25$, $P=0.00241$), and ginsenoside Re and MA and time points (mitochondrial protein carbonyl: $F_{4,\ 250}=3.014$, $P=0.0187$; cytosolic HNE: $F_{4,\ 250}=2.59$, $P=0.0374$). A post hoc test revealed that MA-induced changes in HNE level over time (cytosolic HNE: at 2 h, $P=1.39\times10^{-7}$; at 6 h, $P=5.20\times10^{-24}$; at 1 day, $P=5.74\times10^{-17}$; at 3 days, $P=1.08\times10^{-4}$; at 14 days, $P=0.356$ vs. corresponding Sal + Sal/mitochondrial HNE: at 2 h, $P=1.59\times10^{-9}$; at 6 h, $P=3.05\times10^{-40}$; at 1 day, $P=3.48\times10^{-18}$; at 3 days, $P=1.84\times10^{-6}$; at 14 days, $P=0.0724$ vs. corresponding Sal + Sal) appeared to be comparable to those of protein carbonyl level (cytosolic protein carbonyl: at 2 h, $P=0.100$; at 6 h, $P=3.78\times10^{-25}$; at 1 day, $P=7.35\times10^{-19}$; at 3 days, $P=2.66\times10^{-9}$; at 14 days, $P=0.299$ vs. corresponding Sal + Sal/mitochondrial protein carbonyl: at 2 h, $P=0.147$; at 6 h, $P=2.11\times10^{-23}$; at 1 day, $P=6.20\times10^{-21}$; at 3 days, $P=1.80\times10^{-7}$; at 14 days, $P=0.661$ vs. corresponding Sal + Sal) in the PKCδ (+/+) mice. A significant increase in protein carbonyl or HNE was most pronounced in PKCδ (+/+) mice 6 h after the final MA administration. Both increases remained elevated 3 days after the last MA treatment. However, both increases returned to near control level 14 days later. The increase in mitochondria was more prominent than that in the cytosol. MA-induced oxidative stress was much less pronounced (cytosolic protein carbonyl: at 6 h, $P=2.45\times10^{-7}$; at 1 day, $P=8.63\times10^{-5}$; at 3 days, $P=0.0145$/mitochondrial protein carbonyl: at 6 h, $P=1.81\times10^{-14}$; at 1 day, $P=2.19\times10^{-11}$; at 3 days, $P=0.0149$/cytosolic HNE: at 2 h, $P=0.0163$; at 6 h, $P=5.04\times10^{-5}$; at 1 day, $P=2.67\times10^{-7}$/mitochondrial HNE: at 2 h, $P=0.0132$; at 6 h, $P=3.35\times10^{-22}$; at 1 day, $P=9.15\times10^{-7}$) in PKCδ (−/−) mice than in PKCδ (+/+) mice. Treatment with ginsenoside Re (20 mg/kg, p.o.) significantly attenuated (cytosolic protein carbonyl: at 6 h, $P=4.92\times10^{-5}$; at 1 day, $P=3.02\times10^{-4}$; at 3 days, $P=0.0492$/mitochondrial protein carbonyl: at 6 h, $P=2.99\times10^{-10}$; at 1 day, $P=2.64\times10^{-7}$; at 3 days, $P=0.0496$/cytosolic HNE: at 6 h, $P=2.44\times10^{-6}$; at 1 day, $P=5.28\times10^{-8}$/mitochondrial HNE: at 2 h, $P=0.00278$; at 6 h, $P=1.99\times10^{-16}$; at 1 day, $P=2.12\times10^{-4}$) MA-induced oxidative stress in the cytosolic and mitochondrial fractions of PKCδ (+/+) mice. Ginsenoside Re did not significantly affect attenuation by PKCδ gene knockout against MA toxicity (Fig. 3a–d).

Differential effects of MA on SOD and GPx activity in the cytosol and the mitochondrial fractions were investigated to explore the antioxidant effects mediated by ginsenoside Re or

Fig. 3 Effect of ginsenoside Re on oxidative damage [protein oxidation (carbonyl) and lipid peroxidation (*HNE*)] and antioxidant enzyme activity [superoxide dismutase (*SOD*) and glutathione peroxidase (*GPx*)] induced by methamphetamine (*MA*) in the cytosol and mitochondria of striatum in PKCδ (+/+) and PKCδ (−/−) mice. **a**–**b** Effects on cytosolic and mitochondrial formations of protein carbonyl induced by MA. **c**–**d** Effects on cytosolic and mitochondrial formations of HNE induced by MA. *Sal* saline, *Re (10)* ginsenoside Re (10 mg/kg, p.o.), *Re (20)* ginsenoside Re (20 mg/kg, p.o.). Each value is the mean ± S.E.M. of six animals. *P* values were shown below the figure (four-way ANOVA followed by multiple pairwise comparisons with Bonferroni's correction). **e**–**f** Effects on cytosolic and mitochondrial activity of SOD induced by MA. **g**–**h** Effects on cytosolic and mitochondrial activity of GPx induced by MA. Each value is the mean ± S.E.M. of six animals. $^{*}P<0.05$, $^{**}P<0.01$ vs. corresponding Sal + Sal; $^{\#}P<0.05$, $^{\#\#}P<0.01$ vs. PKCδ (+/+)/Sal + MA (three-way ANOVA followed by multiple pairwise comparisons with Bonferroni's correction)

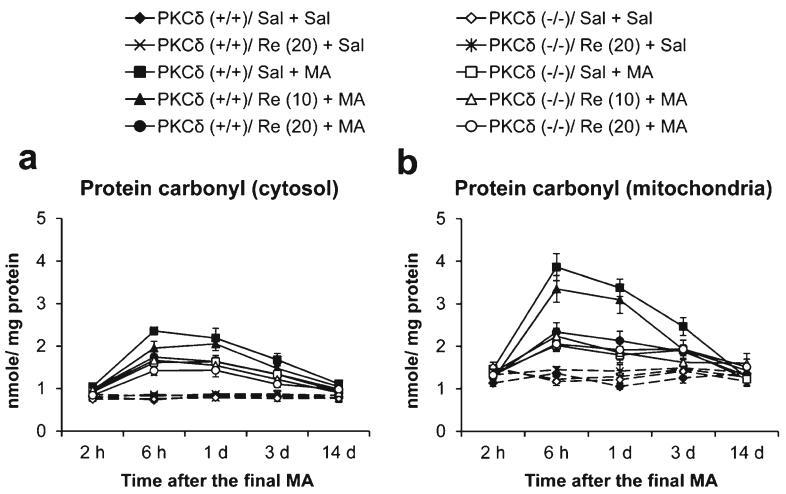

	Protein carbonyl (cytosol)				
	2 h	6 h	1 d	3 d	14 d
PKCδ (+/+)/ Sal + Sal vs. Sal + MA	$P > 0.05$	**$P < 0.01$**	**$P < 0.01$**	**$P < 0.01$**	$P > 0.05$
PKCδ (-/-)/ Sal + Sal vs. Sal + MA	$P > 0.05$	**$P < 0.01$**	**$P < 0.01$**	**$P < 0.01$**	$P > 0.05$
PKCδ (+/+)/ Re (20) + MA vs. Sal + MA	$P > 0.05$	**$P < 0.01$**	**$P < 0.01$**	**$P < 0.05$**	$P > 0.05$
PKCδ (-/-)/ Sal + MA vs. PKCδ (+/+)/ Sal + MA	$P > 0.05$	**$P < 0.01$**	**$P < 0.01$**	**$P < 0.05$**	$P > 0.05$
	Protein carbonyl (mitochondria)				
	2 h	6 h	1 d	3 d	14 d
PKCδ (+/+)/ Sal + Sal vs. Sal + MA	$P > 0.05$	**$P < 0.01$**	**$P < 0.01$**	**$P < 0.01$**	$P > 0.05$
PKCδ (-/-)/ Sal + Sal vs. Sal + MA	$P > 0.05$	**$P < 0.01$**	**$P < 0.05$**	**$P < 0.05$**	$P > 0.05$
PKCδ (+/+)/ Re (20) + MA vs. Sal + MA	$P > 0.05$	**$P < 0.01$**	**$P < 0.01$**	**$P < 0.05$**	$P > 0.05$
PKCδ (-/-)/ Sal + MA vs. PKCδ (+/+)/ Sal + MA	$P > 0.05$	**$P < 0.01$**	**$P < 0.01$**	**$P < 0.05$**	$P > 0.05$

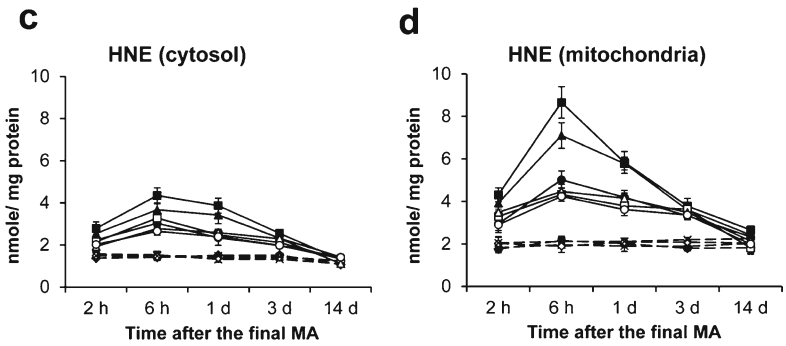

	HNE (cytosol)				
	2 h	6 h	1 d	3 d	14 d
PKCδ (+/+)/ Sal + Sal vs. Sal + MA	**$P < 0.01$**	**$P < 0.01$**	**$P < 0.01$**	**$P < 0.01$**	$P > 0.05$
PKCδ (-/-)/ Sal + Sal vs. Sal + MA	**$P < 0.05$**	**$P < 0.01$**	**$P < 0.01$**	**$P < 0.01$**	$P > 0.05$
PKCδ (+/+)/ Re (20) + MA vs. Sal + MA	$P > 0.05$	**$P < 0.01$**	**$P < 0.01$**	$P > 0.05$	$P > 0.05$
PKCδ (-/-)/ Sal + MA vs. PKCδ (+/+)/ Sal + MA	**$P < 0.05$**	**$P < 0.01$**	**$P < 0.01$**	$P > 0.05$	$P > 0.05$
	HNE (mitochondria)				
	2 h	6 h	1 d	3 d	14 d
PKCδ (+/+)/ Sal + Sal vs. Sal + MA	**$P < 0.01$**	**$P < 0.01$**	**$P < 0.01$**	**$P < 0.01$**	$P > 0.05$
PKCδ (-/-)/ Sal + Sal vs. Sal + MA	**$P < 0.01$**	**$P < 0.01$**	**$P < 0.01$**	**$P < 0.01$**	$P > 0.05$
PKCδ (+/+)/ Re (20) + MA vs. Sal + MA	**$P < 0.01$**	**$P < 0.01$**	**$P < 0.01$**	$P > 0.05$	$P > 0.05$
PKCδ (-/-)/ Sal + MA vs. PKCδ (+/+)/ Sal + MA	**$P < 0.05$**	**$P < 0.01$**	**$P < 0.01$**	$P > 0.05$	$P > 0.05$

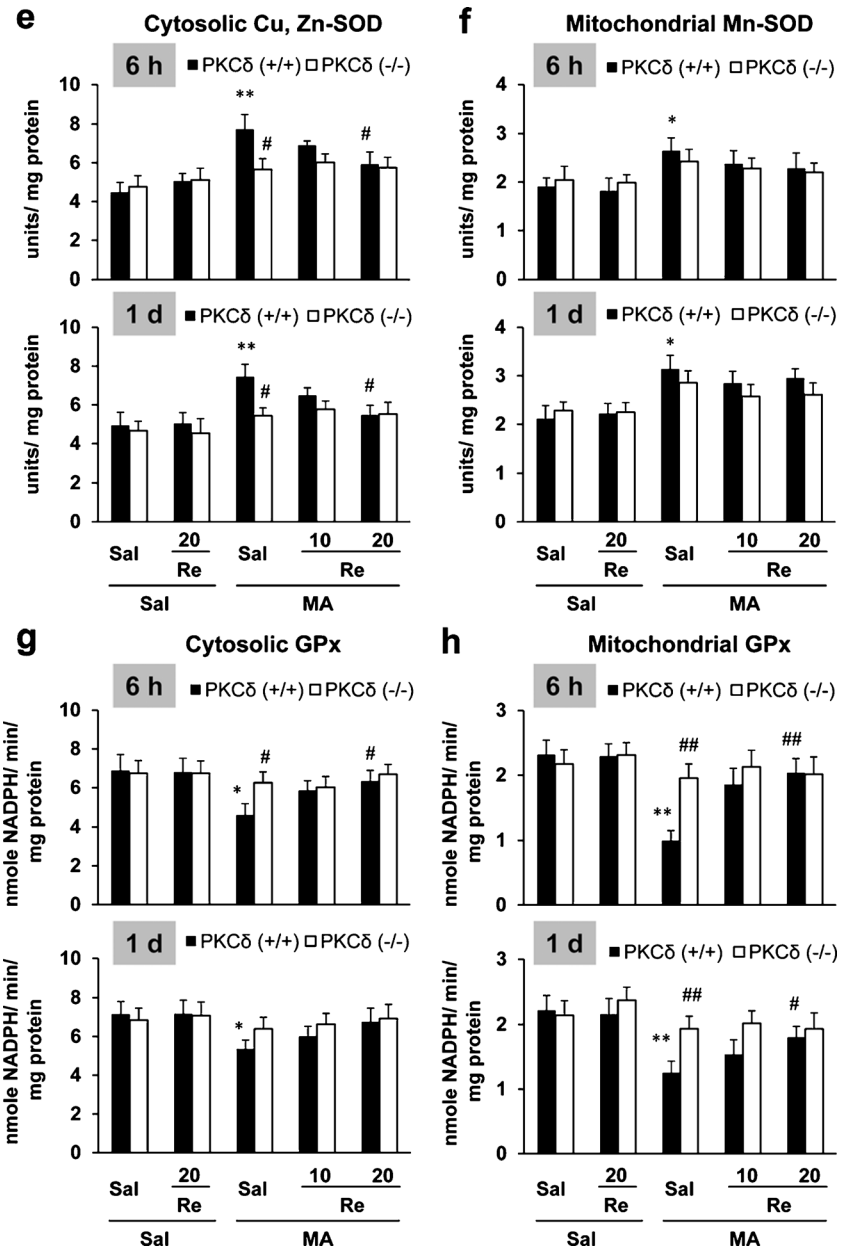

Fig. 3 (continued)

PKCδ gene knockout. Consistent with prior reports [51, 52], striatal GPx activity was higher in the cytosol than in the mitochondrial fractions.

In the absence of MA, there was no significant difference between PKCδ (+/+) and PKCδ (−/−) mice in terms of either SOD or GPx activity in the cytosolic and mitochondrial fractions. Since MA-induced changes in SOD and GPx activities were observed primarily at 6 h and 1 day after the last MA treatment, we focused on these two time points to determine whether ginsenoside Re or PKCδ gene knockout selectively modulated mitochondrial enzymatic activity of SOD and GPx. MA-induced increases in cytosolic Cu, Zn-SOD activity (6 h or 1 day; $P<0.01$ vs. corresponding Sal + Sal) were more pronounced than mitochondrial Mn-SOD activity (6 h or 1 day; $P<0.05$ vs. corresponding Sal + Sal) in the PKCδ (+/+) mice. Ginsenoside Re (6 h or 1 day; $P<0.05$ vs. corresponding Sal + MA) or PKCδ gene knockout (6 h or 1 day; $P<0.05$ vs. corresponding Sal + MA) significantly attenuated these increases in cytosolic Cu, Zn-SOD activity in the PKCδ (+/+) mice. However, neither ginsenoside Re nor PKCδ gene knockout significantly altered mitochondrial Mn-SOD activity (Fig. 3e, f).

In contrast, MA-induced significant decreases in cytosolic (6 h or 1 day; $P<0.05$ vs. corresponding Sal + Sal) and mitochondrial GPx activities (6 h or 1 day; $P<0.01$ vs. corresponding

saline + saline) in PKCδ (+/+) mice. The MA-induced decrease in GPx activity was more prominent in the mitochondrial fraction than in the cytosolic fraction. Ginsenoside Re (mitochondrial fraction: 6 h; $P<0.01$ or 1 day; $P<0.05$ vs. corresponding Sal + MA; cytosolic fraction: 6 h; $P<0.05$ vs. corresponding Sal + MA) or PKCδ gene knockout (mitochondrial fraction: 6 h, or 1 day; $P<0.01$ vs. corresponding Sal + MA; cytosolic fraction: 6 h; $P<0.05$ vs. corresponding Sal + MA) significantly attenuated decreases in GPx activity induced by MA in PKCδ (+/+) mice (Fig. 3g, h). Thus, it is possible that ginsenoside Re or PKCδ gene knockout is more effective in modulating GPx activity than in modulating SOD activity and that the effect of ginsenoside Re or PKCδ gene knockout might be more specific for mitochondrial GPx activity than cytosolic GPx activity in the presence of MA.

Protective Effects of Ginsenoside Re on MA-Induced Changes in Mitochondrial Membrane Potential and Intramitochondrial Ca^{2+} Level Mediated by PKCδ

A previous study demonstrated that disturbed Ca^{2+} homeostasis may mediate dopaminergic degeneration, such as PD [53]. We examined whether genetically inhibiting PKCδ would affect mitochondrial membrane potential and intramitochondrial Ca^{2+} accumulation in the striatum of PKCδ (+/+) mice.

As the MA-induced increase in mitochondrial oxidative damage was most pronounced 6 h after the final MA treatment in the striatum of PKCδ (+/+) mice (refer to Fig. 3a–d), we selected this time point for further study. As shown in Fig. 4a, b, mitochondrial membrane potential and intramitochondrial Ca^{2+} remained unchanged in the absence of MA. Treatment with MA resulted in a significant decrease ($P<0.01$) in mitochondrial membrane potential in PKCδ (+/+) mice, whereas MA treatment significantly increased ($P<0.01$) intramitochondrial Ca^{2+}. However, these changes were not observed in PKCδ (−/−) mice. Ginsenoside Re treatment significantly attenuated (mitochondrial membrane potential, $P<0.05$; intramitochondrial Ca^{2+}, $P<0.01$) these morbid changes in PKCδ (+/+) mice. Ginsenoside Re treatment did not significantly alter these parameters observed in MA-treated PKCδ (−/−) mice, suggesting that PKCδ is a critical target for the protective activity of ginsenoside Re in response to mitochondrial dysfunction induced by MA (Fig. 4a, b).

Protective Effects of Ginsenoside Re on MA-Induced Mitochondrial Translocation of PKCδ in the Striatum of the Mice

We recently demonstrated that PKCδ mediates MA-induced dopaminergic neurotoxicity in vivo [25, 26]. However, the significance of mitochondrial translocation of PKCδ remains unknown in this condition.

In the striatum of PKCδ (+/+) mice, mitochondrial translocation of cleaved PKCδ was most evident ($P<0.01$) 1 day after the final injection of MA (Supplementary Fig. 2). Therefore, we chose this time point for further study. Treatment with MA resulted in significant increases ($P<0.01$ vs. Sal + Sal) in the cytosolic expression of PKCδ and cleaved PKCδ and their mitochondrial translocation. These changes were significantly attenuated by ginsenoside Re (cytosolic and mitochondrial PKCδ: ginsenoside Re 20 mg/kg + MA vs. Sal + MA, $P<0.05$; cytosolic and mitochondrial cleaved PKCδ: ginsenoside Re 10 or 20 mg/kg + MA vs. Sal + MA: $P<0.05$ or $P<0.01$) (Fig. 4c).

Protective Effects of Ginsenoside Re on MA-Induced Microglial Activation Mediated by PKCδ in the Striatum of Mice

Accumulating evidence suggests that mitochondrial damage links inflammation to neuronal death [54]. Further, it is recognized that the role of glial cells in MA-induced neurotoxicity is essential to identify factors contributing or mitigating MA-induced damage to DA nerve terminals. Importantly, it has been proposed that microglia participate in neurotoxicity associated with MA intoxication [38, 55–58]. In this study, we examined activated patterns of microglia and astrocytes induced by MA in the striatum and SN. MA treatment activated Iba-1-positive microglia in the striatum (1 and 3 days post-MA, $P<0.01$ vs. Sal). This activation at 1 day was more evident than at 3 days after the last MA treatment. This microglial activation at 1 day post-MA was approximately comparable to that at 1 day post-MPTP ($P<0.01$ vs. Sal). MA treatment did not significantly alter Iba-1-positive microglia in the SN, even though MPTP treatment significantly activated microglia in the same area ($P<0.01$ vs. Sal; Fig. 5a).

In contrast, significant activation of GFAP-positive astrocytes induced by MA was observed in the striatum (1 and 3 days post-MA, $P<0.01$ vs. saline) and SN (1 day post-MA, $P<0.05$; 3 days post-MA, $P<0.01$ vs. saline). Activation of GFAP-positive astrocytes in nigral area was more prominent than in the striatal area. These reactive astrocytes in the nigrostriatal regions were more pronounced in the mice-treated with MPTP ($P<0.01$ vs. saline) than those-treated with MA (Fig. 5b). We subsequently examined effects of ginsenoside Re or PKCδ inhibition in response to striatal activation of Iba-1-positive microglia induced by MA. MA-induced microglial activation was significantly attenuated (1 day post-MA, $P<0.01$; 3 days post-MA, $P<0.05$ vs. corresponding Sal + MA) by ginsenoside Re in PKCδ (+/+) mice. This attenuation by ginsenoside Re was comparable to that seen with genetic inhibition of PKCδ (1 day post-MA, $P<0.01$; 3 days post-MA, $P<0.05$ vs. corresponding Sal + MA). However, ginsenoside Re did not affect the attenuation in MA-treated PKCδ (−/−) mice (Fig. 5c, d).

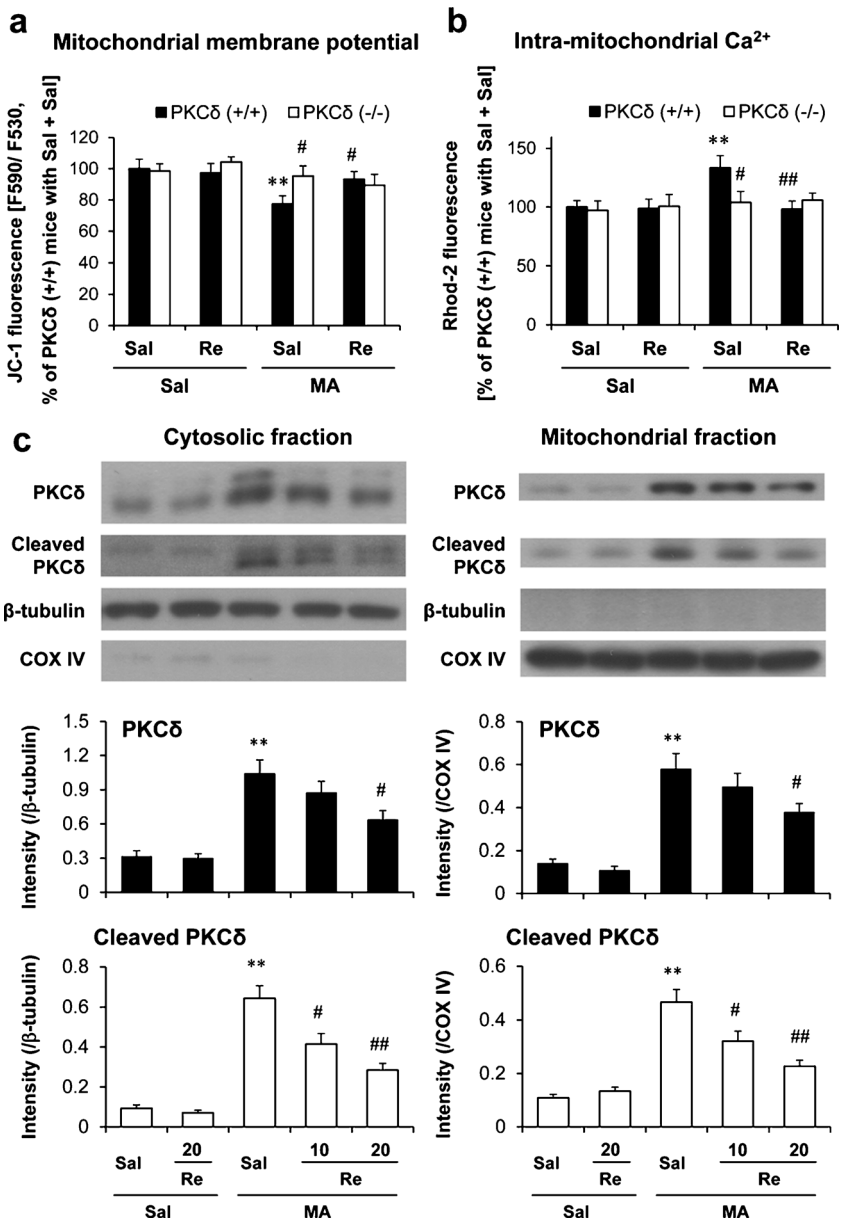

Fig. 4 Effect of ginsenoside Re on methamphetamine (*MA*)-induced mitochondrial dysfunction and mitochondrial translocation of PKCδ. **a** Effects on mitochondrial membrane potential 6 h after the final MA injection in the striatum of PKCδ (+/+) and PKCδ (−/−) mice. **b** Effects on intramitochondrial Ca^{2+} level 6 h after the final MA injection in the striatum of PKCδ (+/+) and PKCδ (−/−) mice. See text for details. *Sal* saline, *Re* ginsenoside Re (20 mg/kg, p.o.). Each value is the mean ± S.E.M. of four experiments (striatal mitochondria from five animals pooled for each assay). $^{**}P<0.01$ vs. corresponding group/Sal + Sal; $^{\#}P<0.05$, $^{\#\#}P<0.01$ vs. PKCδ SO or PKCδ (+/+)/Sal + MA (three-way ANOVA followed by multiple pairwise comparisons with Bonferroni's correction). **c** Effects on MA-induced changes in the cytosolic expression of PKCδ and cleaved PKCδ and their mitochondrial translocation in the striatum of PKCδ (+/+) mice. Each value is the mean ± S.E.M. of six animals. $^{**}P<0.01$ vs. Sal + Sal; $^{\#}P<0.05$, $^{\#\#}P<0.01$ vs. Sal + MA (two-way ANOVA followed by multiple pairwise comparisons with Bonferroni's correction)

It has been suggested that macrophages/microglia play different roles in tissue repair or damage in response to CNS injury [59–63]. These divergent effects may be due to distinct macrophage/microglial subsets, i.e., "classically activated" pro-inflammatory (M1) or "alternatively activated" anti-inflammatory (M2) cells. MA treatment significantly enhanced the mRNA level of M1 markers (1 and 3 days post-MA; CD16, CD32, or CD86: $P<0.01$ vs. corresponding Sal + Sal) in PKCδ (+/+) mice, and mRNA levels of M2 markers were not significantly decreased. These results indicated that microglia after MA treatment existed primarily in the classically activated state, which is highly pro-inflammatory. Treatment with ginsenoside Re resulted in significant attenuation in response to MA-induced increased mRNA expression of M1 markers (1 day post-MA; CD16: $P<0.01$, CD32 or CD86: $P<0.05$ vs. corresponding Sal + MA; 3 days post-MA; CD16, CD32, or CD86: $P<0.05$ vs. corresponding Sal + MA). This attenuation by ginsenoside Re on PKCδ (+/+) mice was comparable to that by PKCδ knockout in the presence of MA (Fig. 5e–i). Therefore, ginsenoside Re or genetic inhibition of PKCδ may dampen this neuroinflammatory process.

Protective Effects of Ginsenoside Re on MA-Induced Increase in TUNEL-Positive Neurons Mediated by PKCδ in the Striatum of Taconic ICR Mice

PKCδ is an oxidative stress-sensitive kinase and its activation via caspase-3-dependent proteolysis induces apoptotic cell death in cell culture model of PD [23]. We were interested in

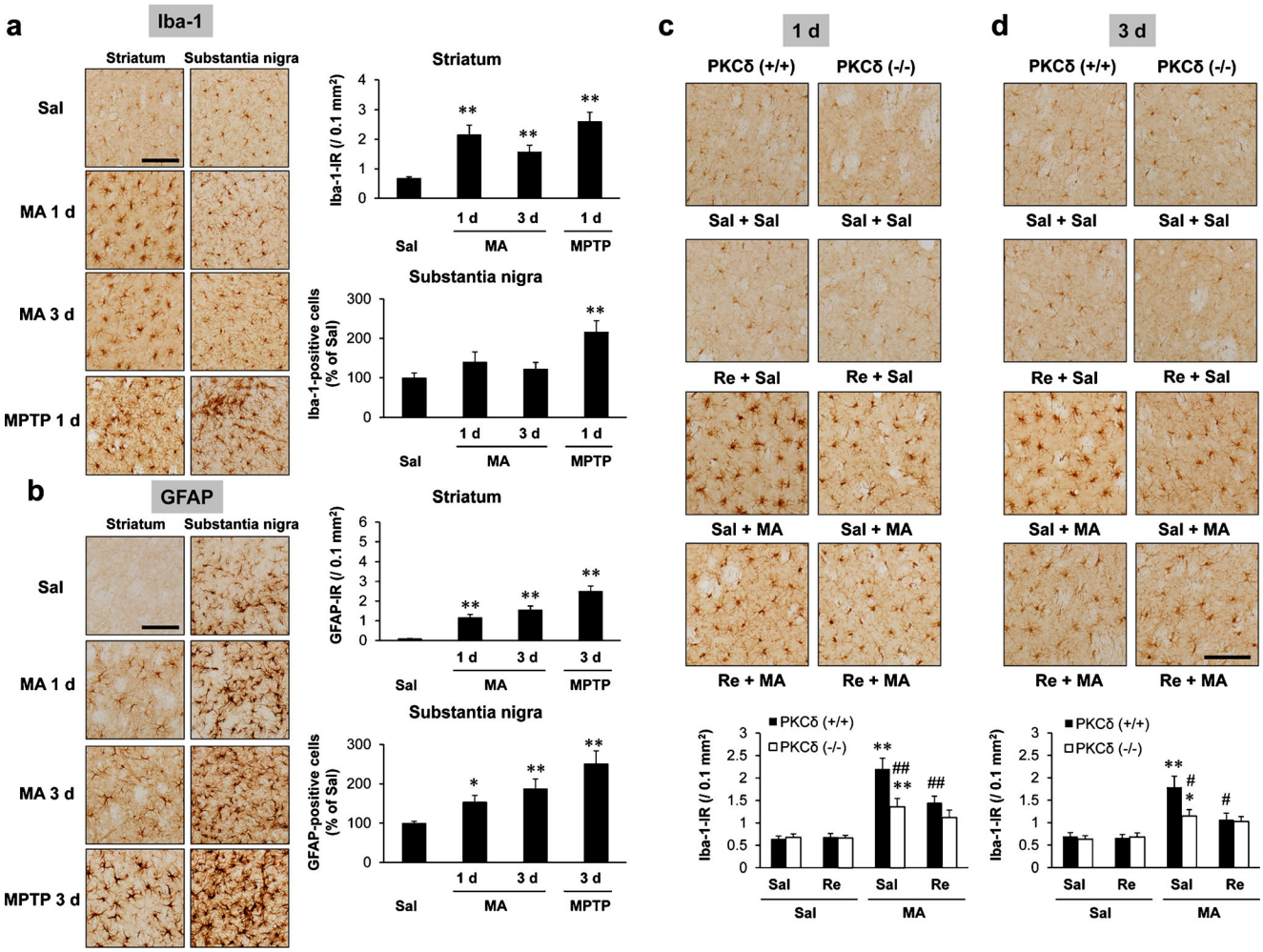

Fig. 5 Effect of ginsenoside Re on methamphetamine (*MA*)-induced microglial activation in the striatum of PKCδ (+/+) and PKCδ (−/−) mice. **a** MA-induced changes in Iba-1-immunoreactive microglia in the striatum and substantia nigra (*SN*) of the PKCδ (+/+) mice compared with MPTP. **b** MA-induced changes in GFAP-immunoreactive astrocytes in the striatum and SN of the PKCδ (+/+) mice compared with MPTP. **c** Effect on Iba-1-immunoreactive microglial activation 1 day after the last MA treatment in the striatum. **d** Effect on Iba-1-immunoreactive microglial activation 3 days after the last MA treatment in the striatum. **e**–**g** Effect on microglial differentiation into M1 type after the last MA treatment. **h**–**i** Effect on microglial differentiation into M2 type after the last MA treatment. Each value is the mean ± S.E.M. of five animals. $^{*}P<0.05$, $^{**}P<0.05$ vs. corresponding Sal or Sal + Sal; $^{\#}P<0.05$, $^{\#\#}P<0.01$ vs. PKCδ (+/+)/Sal + MA [one-way ANOVA (**a** and **b**) or three-way ANOVA (**c**–**i**) followed by multiple pairwise comparisons with Bonferroni's correction]. *Scale bar*=100 μm

whether ginsenoside Re would affect this apoptotic signaling pathway after MA exposure.

Earlier reports demonstrated that MA induces apoptotic cell death in striatal neurons [64]. In the present study, we chose TUNEL staining (which labels the occurrence of DNA fragmentation, which occurs late in apoptosis). We previously failed to observe MA-induced TUNEL-positive cells in the striatum of PKC (+/+) mice 12 h, 1 day, or 3 days after the final MA administration (i.e., four injections of 8 mg/kg MA, intraperitoneally at 2 h intervals or a single injection of MA [20–40 mg/kg]), suggesting that the C57BL/6 background is not sensitive to TUNEL staining [26, 65]. Thus, according to previous reports [26, 29, 30], we used 10-week-old male Taconic ICR mice. Because apoptotic cell death was detectable at 20 mg/kg MA and reached a significant level at 35 mg/kg in our previous study, a 35-mg/kg dose of MA was chosen for the present study. We also sacrificed animals 1 day after MA administration [26, 29, 30], and TUNEL-positive cells were induced maximally at this time point.

Figure 6 shows representative photomicrographs of TUNEL-positive cells in the striatum of MA-treated mice. Very few TUNEL-positive cells were observed in the absence of MA. Neither ginsenoside Re, PKCδ ASO, nor ginsenoside Re with PKCδ ASO significantly induced TUNEL-positive cells. The MA-induced increase in the number of TUNEL-positive cells was much less pronounced ($P<0.01$) in the PKCδ ASO-treated mice than in the PKCδ SO-treated mice. Treatment with ginsenoside Re significantly attenuated

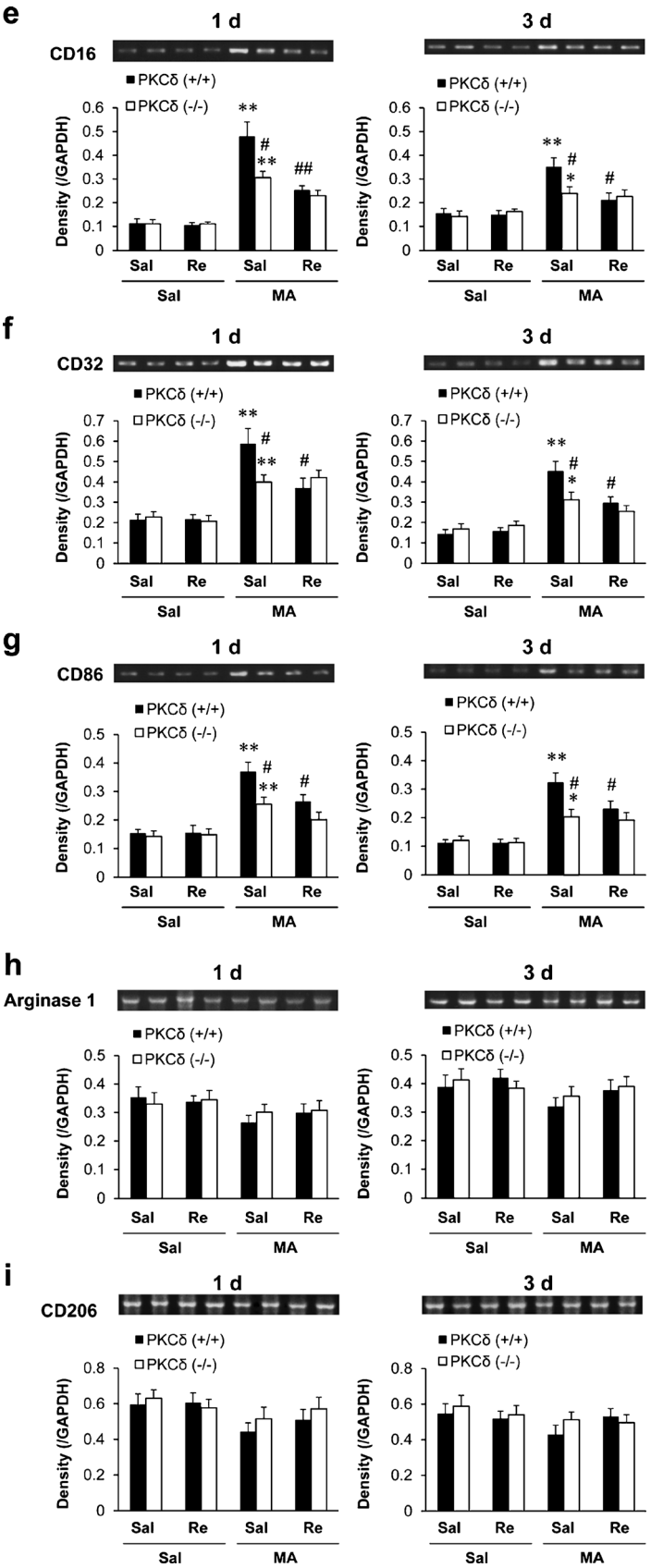

Fig. 5 (continued)

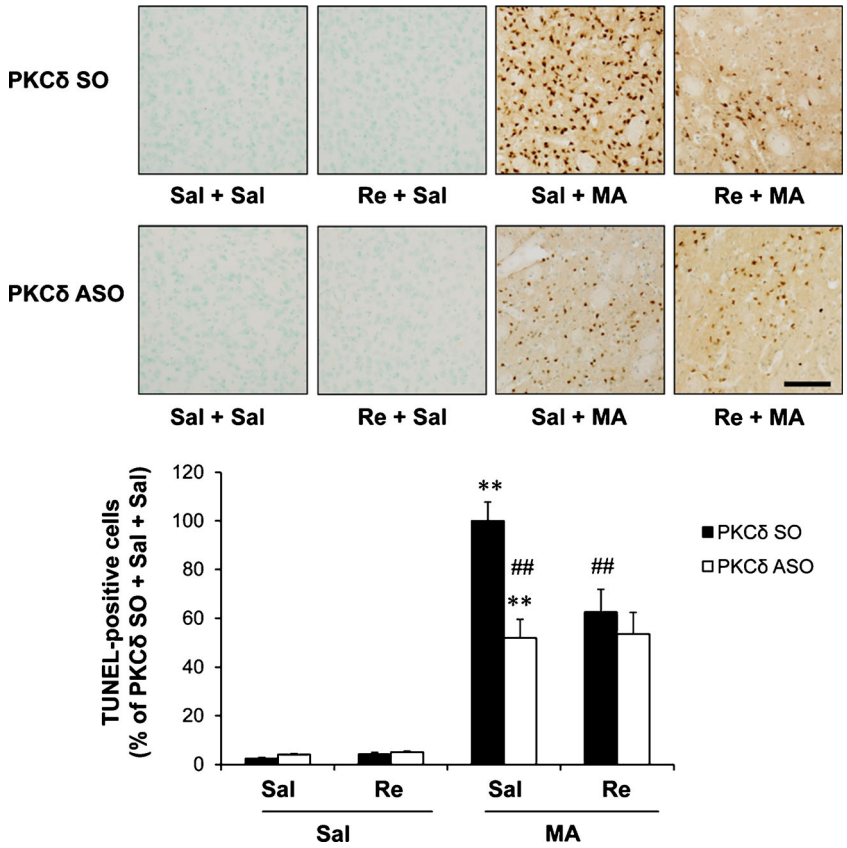

Fig. 6 Effect of ginsenoside Re on the pro-apoptotic changes induced by methamphetamine (*MA*). Effect on MA (35 mg/kg, i.p. × 1)-induced increase in TUNEL-positive cells in the striatum of the Taconic ICR mice in the presence of PKCδ SO or PKCδ ASO. PKCδ SO or PKCδ ASO was microinfused into the lateral ventricle at a dose of 2.5 μg/μL. *Re* ginsenoside Re (20 mg/kg, p.o.). Each value is the mean ± S.E.M. of six animals. $^{**}P<0.01$ vs. corresponding group/Sal + Sal; $^{\#\#}P<0.01$ vs. PKCδ SO + Sal (three-way ANOVA followed by multiple pairwise comparisons with Bonferroni's correction). *Scale bar*=100 μm

($P<0.01$) the increase in TUNEL-positive cells induced by MA in PKCδ SO-treated mice but did not significantly alter the attenuating effects by PKCδ ASO against MA insult.

Protective Effects of Ginsenoside Re on MA-Induced Decrease in Dopamine Level and TH Values (Immunodistribution, Expression, and Activity) Mediated by PKCδ

As shown in Fig. 7a, an initial decrease in striatal dopamine level was observed 2 h after the final MA treatment of PKCδ (+/+) mice. This decrease lasted for at least 14 days. The ANOVA indicated significant effects of PKCδ gene knockout ($F_{1,\ 200}=10.21$, $P=0.00162$), MA ($F_{1,\ 200}=189.89$, $P=8.20\times10^{-31}$), and ginsenoside Re ($F_{1,\ 200}=8.23$, $P=0.00455$) and significant interactions between PKCδ gene knockout and MA ($F_{1,\ 200}=6.87$, $P=0.00947$), ginsenoside Re and MA ($F_{1,\ 200}=5.60$, $P=0.0189$), and PKCδ gene knockout and ginsenoside Re and MA ($F_{1,\ 200}=6.09$, $P=0.0144$). A post hoc test revealed that the MA-induced decrease (at 2 h, $P=0.00240$; at 6 h, $P=1.71\times10^{-5}$; at 1 day, $P=1.45\times10^{-6}$; at 3 days, $P=6.65\times10^{-9}$; at 14 days, $P=4.23\times10^{-7}$ vs. corresponding Sal + Sal) in dopamine level was most pronounced 3 days after the final MA treatment in PKCδ (+/+) mice. Ginsenoside Re treatment resulted in significant attenuations (at 1 day, $P=0.0151$; at 3 days, $P=0.00506$; at 14 days, $P=0.0312$ vs. Sal + MA) over time in response to MA-induced decreases in dopamine level in PKCδ (+/+) mice. The decrease in PKCδ (−/−) mice was much less pronounced [at 1 day, $P=0.0392$; at 3 days, $P=0.00159$; at 14 days, $P=0.0126$ vs. PKCδ (+/+)] over time than that in PKCδ (+/+) mice. Ginsenoside Re treatment did not significantly affect attenuation mediated by PKCδ gene knockout.

As the decrease in dopamine level was most pronounced 3 days after the final MA treatment, we examined TH protein expression, TH immunodistribution (TH-IR: immunostaining), and TH activity at that time. Striatal TH expression was not affected in the absence of MA in either PKCδ (+/+) or PKCδ (−/−) mice. MA treatment significantly decreased ($P<0.01$) TH expression in PKCδ (+/+) mice. This decrease was significantly protected by ginsenoside Re ($P<0.01$) or PKCδ gene knockout ($P<0.01$). Ginsenoside Re did not affect attenuation by PKCδ gene knockout. The decrease in striatal TH-IR was consistently comparable to that of nigral TH-IR. A significant MA-induced decrease in nigrostriatal TH-IR ($P<0.01$) was observed in PKCδ (+/+) mice. These dopaminergic parameters consistently paralleled the profile of striatal TH activity. The MA-induced decrease in these dopaminergic parameters was significantly inhibited by ginsenoside Re ($P<0.05$) or by genetically inhibiting PKCδ (nigrostriatal

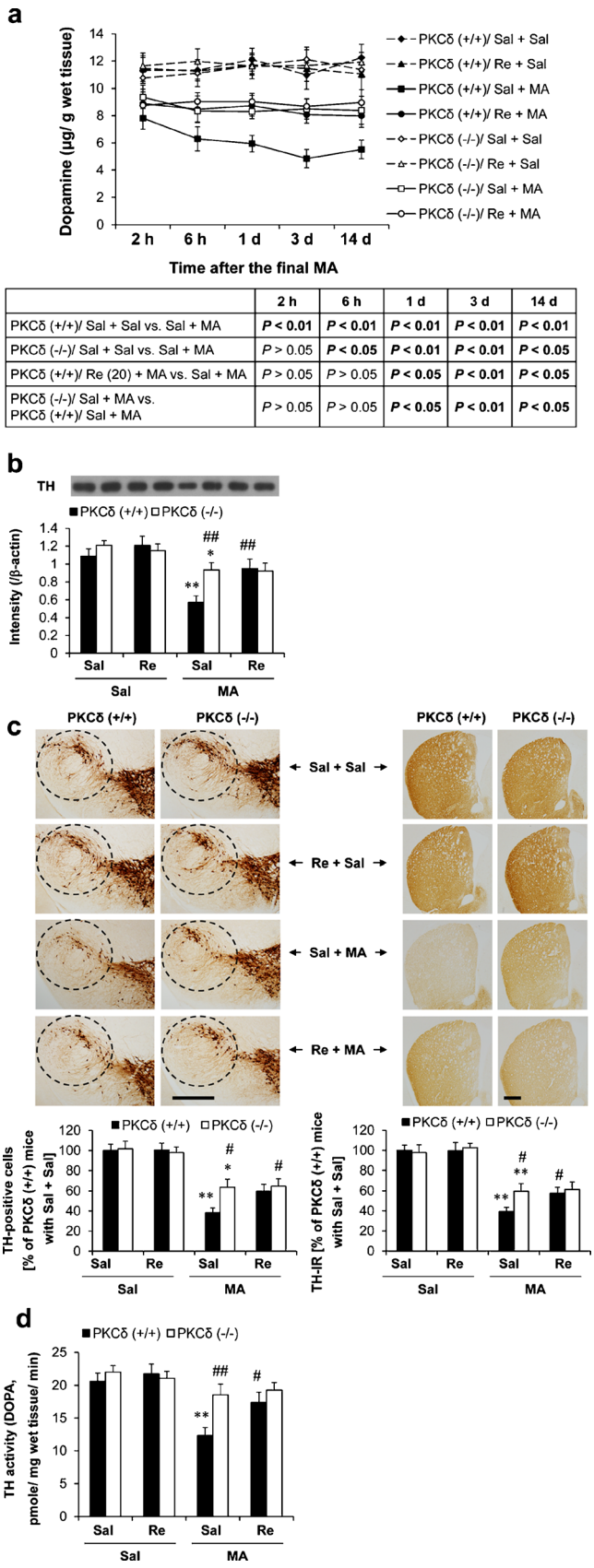

	2 h	6 h	1 d	3 d	14 d
PKCδ (+/+)/ Sal + Sal vs. Sal + MA	***P* < 0.01**	***P* < 0.01**	***P* < 0.01**	***P* < 0.01**	***P* < 0.01**
PKCδ (-/-)/ Sal + Sal vs. Sal + MA	*P* > 0.05	***P* < 0.05**	***P* < 0.01**	***P* < 0.01**	***P* < 0.05**
PKCδ (+/+)/ Re (20) + MA vs. Sal + MA	*P* > 0.05	*P* > 0.05	***P* < 0.05**	***P* < 0.01**	***P* < 0.05**
PKCδ (-/-)/ Sal + MA vs. PKCδ (+/+)/ Sal + MA	*P* > 0.05	*P* > 0.05	***P* < 0.05**	***P* < 0.01**	***P* < 0.05**

Fig. 7 Effect of ginsenoside Re on methamphetamine (*MA*)-induced dopaminergic toxicity. **a** Effect on the decrease in dopamine level over time after the last MA treatment in the striatum of PKCδ (+/+) and PKCδ (−/−) mice. Each value is the mean ± S.E.M. of 5 animals. *P* values were shown *below the figure* (four-way ANOVA followed by multiple pairwise comparisons with Bonferroni's correction). **b**–**d** Effect on decreased striatal TH expression (**b**), nigrostriatal TH-immunoreactivity (**c**), and striatal TH activity (**d**) 3 days after the final MA treatment. *Dotted circles* indicate substantia nigra pars compacta. *Sal* saline, *Re* ginsenoside Re (20 mg/kg, p.o.). Each value is the mean ± S.E.M. of 6~8 animals. $^{*}P<0.05$, $^{**}P<0.01$ vs. corresponding Sal + Sal; $^{\#}P<0.05$, $^{\#\#}P<0.01$ vs. PKCδ (+/+)/Sal + MA (three-way ANOVA followed by multiple pairwise comparisons with Bonferroni's correction). *Scale bar*=500 μm

TH-IR, $P<0.05$; striatal TH activity, $P<0.01$). Ginsenoside Re did not significantly alter attenuation by genetically inhibiting PKCδ (Fig. 7b–d).

Protective Effects of Ginsenoside Re on MA-Induced Behavioral Impairments Mediated by PKCδ

Due to the similarities between neurotoxic profiles of high-dose MA treatment and PD in humans, it was confirmed that neurotoxic doses of MA lead to motor disturbances in rodents [66]. We have demonstrated that neurotoxic doses of MA produce behavioral impairments and that these impairments are significantly inhibited by pharmacologically or genetically inhibiting PKCδ [25, 26]. We conducted a time-course study to understand changes in behavioral activity after the last MA administration.

As shown in Fig. 8a, a significant reduction ($P<0.01$ vs. corresponding Sal + Sal) in locomotor activity was observed initially 1 day after the final MA dose. This hypolocomotor activity lasted for at least 14 days. The ginsenoside Re treatment significantly attenuated ($P<0.05$) this decrease in PKCδ (+/+) mice over time. The attenuation by ginsenoside Re was comparable to that by PKCδ gene knockout ($P<0.05$). Ginsenoside Re treatment did not significantly alter the attenuation by PKCδ gene knockout. The profile of locomotor activity under our experimental conditions paralleled that of a rotarod (Fig. 8b).

Discussion

We and others have shown that ginsenosides have antagonistic effects on the neurochemical and psychoneurological toxicity of MA. For example, ginsenosides attenuate MA-induced dopaminergic dysfunction/neurotoxicity [67–69] and inhibit MA-induced behavioural side effects [27, 67]. In addition, ginsenoside-mediated neuroprotective effects are related to antioxidant potential by attenuating synaptosomal and mitochondrial oxidative stressor, mitochondrial dysfunction [37, 70].

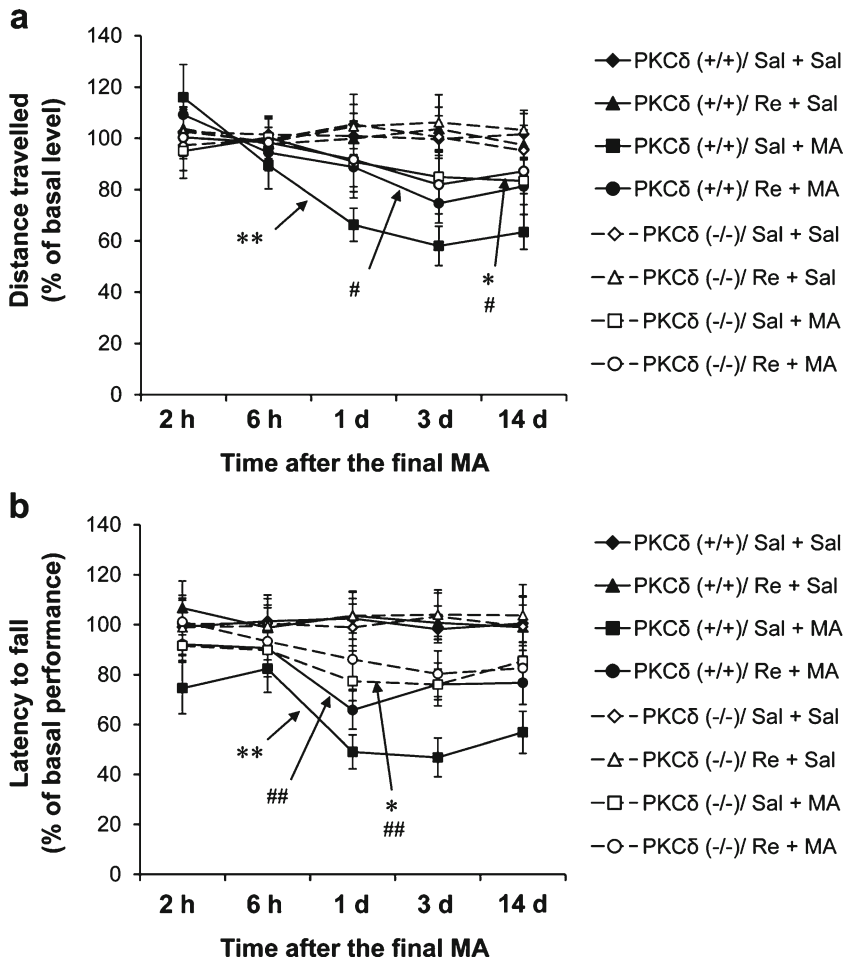

Fig. 8 Effect of ginsenoside Re on methamphetamine (MA)-induced behavioral impairment over time in PKCδ (+/+) and PKCδ (−/−) mice. **a**. Effect on MA-induced reduced locomotor activity. **b**. Effect on MA-induced reduced rota-rod performance. *Sal* saline, *Re* ginsenoside Re (20 mg/kg, p.o.). Each value is the mean ± S.E.M. of 10 animals. $^{*}P<0.05$, $^{**}P<0.01$ vs. corresponding Sal + Sal; $^{\#}P<0.05$, $^{\#\#}P<0.01$ vs. PKCδ (+/+)/Sal + MA (repeated measure four-way ANOVA followed by multiple pair-wise comparisons with Bonferroni's correction)

Lopez et al. [71] demonstrated that ginsenoside Re significantly attenuates astrocytic death and oxidative stress generated by H_2O_2, suggesting its potential antiapoptotic and antioxidant effects. In addition, ginsenoside Re inhibits 12-*O*-tetradecanoylphorbol-13-acetate (TPA)-induced inflammation and macrophage activation [72]. Importantly, PKC is a major intracellular receptor for TPA that can activate classical and novel PKC isoforms [73] such as PKCδ, which is an oxidative stress-sensitive kinase whose activation induces apoptotic cell death via inflammatory apoptosis in PD models [22–24]. In addition, PKCδ is highly expressed in the striatum and SN of the brain [22]. Its expression increases with age [74] and is a risk factor for PD [75]. Importantly, increased incidence of PD among individuals with a history of amphetamine use has been reported [76, 77].

Multiple MA doses do not significantly alter PKCα, PKCβI, PKCβII, or PKCζ expression in the striatum, but do significantly and selectively increase PKCδ expression [26]. Furthermore, MA-induced enhancement of PKCδ expression is a critical factor in impaired TH phosphorylation, and pharmacologically or genetically inhibiting PKCδ is protective against MA-induced dopaminergic neurotoxicity in vivo [25].

In this study, MA treatment resulted in significant and constant increases in SOD activity in the striatum of wild-type mice, but did not involve a concomitant increase in GPx activity. Increased SOD activity may lead to an accumulation of H_2O_2, which in the absence of simultaneous increases in the activity of GPx could increase Fenton reactions leading to the stimulation of lipid peroxidation/protein oxidation that results in irreversible cellular damage [50, 78]. In contrast, increased catalase activity in MA-treated wild-type mice could be an adaptive response to higher levels of H_2O_2 generated by inhibition of GPx activity; the brain has low-level catalase activity and only moderate amounts of SOD and GPx [78, 79]. Our observation of increased lipid peroxidation/protein oxidation products implies that GPx activity, rather than increased SOD, modulates these endpoints. Furthermore, significant elevation of cytosolic Cu, Zn-SOD activity in the early stages of MA insult in wild-type mice could be a response to the enhanced superoxide generated during MA-induced neurotoxicity [80, 81]. In other words, enhanced activity of GPx in the presence of ginsenoside Re or PKCδ gene inhibition may be responsible for lowering H_2O_2 levels, which could inactivate SOD.

Although mitochondrial Mn-SOD, in contrast to cytosolic Cu, Zn-SOD, was not highly induced in the striatum, wild-type mice showed increased Mn-SOD activity in the early stages (6 h and 1 day) of MA insult that may be due to the formation of H_2O_2 in the mitochondria [50]. The relationship between mitochondrial damage, glutathione status, oxidative stress, and neuronal dysfunction has been recognized by the effects of excessive production of H_2O_2 within mitochondria, which leads to depletion of mitochondrial GSH, in turn causing reduction of mitochondrial GPx activity and impairment of mitochondrial function [50, 82]. DA in solution undergoes auto-oxidation, resulting in the production of H_2O_2. Indeed, DA auto-oxidation leads to the formation of reactive quinone derivatives and H_2O_2 [83]. Therefore, the protective effect against MA-induced dopaminergic deficits in the presence of ginsenoside Re or PKCδ gene knockout might reflect an anti-peroxidative (mitochondrial > cytosolic) role of GPx.

Our results clearly suggest that MA-induced toxic damage might be more pronounced in the mitochondrial fraction than in the cytosolic fraction in wild-type mice and that ginsenoside Re or genetically inhibiting PKCδ significantly attenuates this oxidative damage, mitochondrial dysfunction, apoptotic changes, dopaminergic impairment (including behavioral impairments), and hyperthermia (Supplementary Fig. 3). Importantly, ginsenoside Re does not significantly alter neuroprotective activity mediated by genetically inhibiting PKCδ, suggesting that PKCδ is a critical target for the neuroprotective activity of ginsenoside Re. This is the first investigation of the role of PKC per se in ginsenoside Re-mediated neuroprotective potential with recovery of mitochondrial function.

Kim et al. [17] demonstrated that significant loss of mitochondrial complex IV activity in PINK1 (related to autosomal recessive forms of familial PD) null dopaminergic neurons. They observed that ginsenoside Re treatment attenuated loss of complex IV and its associated signaling network by restoring optimal NO signaling in PINK1 null cells. Thus, our results are, at least in part, in line with their finding that restoration of mitochondrial function is important for the ginsenoside Re-mediated neuroprotective mechanism.

We propose here that MA potentiates mitochondrial oxidative stress and also impairs mitochondrial detoxification system, mitochondrial membrane potential, possibly due to calcium accumulation. Increased intracellular Ca^{2+} promotes the accumulation of Ca^{2+} within the mitochondrial matrix when total Ca^{2+} uptake exceeds total Ca^{2+} efflux from mitochondria [84]. Mitochondrial Ca^{2+} overload may also lead to the uncoupling of mitochondrial electron transport and may potentiate oxidative stress. Decreases in the mitochondrial membrane potential and increases in oxidative damage after MA treatment could be mediated by Ca^{2+} entry. We speculate that ginsenoside Re might, at least in part, block Ca^{2+} entry through the mitochondrial translocation of PKCδ, given that ginsenoside Re primarily attenuated mitochondrial dysfunction.

Microglial activation and oxidative stress induced by mitochondrial toxins (i.e., 3-nitropropionic acid) caused neuronal loss in the striatum [85]. Mitochondria can be a target of free radical stress initiated by activated microglia. The combination of mitochondrial dysfunction, oxidative stress, and exacerbated activation of microglia generates a vicious cycle that appears to lead to progressive DA neuronal cell death [86]. Previous work demonstrated reactive microglia [87, 88] and increased density of GFAP-positive astrocytes [88] in brains of human MA abusers. Importantly, activation of caspases regulates microglia activation through a PKCδ-dependent pathway [89].

Thomas et al. [55] proposed possible links between MA neurotoxicity and microglial activation, including early changes in microglial associated gene expression. They observed that MA-induced activation of isolectin B_4-positive microglia selectively occurs in the striatum. In contrast, they found that MA produces no evidence of isolectin B_4-positive microglial activation in the SN. MA causes a significant increase in isolectin B_4-positive microglial activation in the striatum 24 to 48 h after the last treatment (MA 5 mg/kg × four times with a 2-h interval) that returned to control levels after 7 days. Our results are consistent with the findings of Thomas and Kuhn [56] and suggest that microglial reactivity remains a specific marker for acute damage to DA terminals following a neurotoxic regimen of MA, even though we followed a different microglial marker (Iba-1) following higher doses of MA (8 mg/kg × four times with a 2-h interval) in this study. In addition, MA treatment significantly increased the mRNA expression of M1 phenotypic markers (CD16, CD32, and CD86), suggesting that microglia after MA treatment existed primarily in the classically activated state [38], which is pro-inflammatory. Thus, our results indicate that neuroprotection by ginsenoside Re or PKCδ inhibition is, at least in part, mediated by its anti-inflammatory properties.

In this study, the selective DA neurotoxin MPTP resulted in extensive microglial and astrocyte activation in the striatum, as well as in the area of the SN. Conversely, in animals treated with MA, GFAP-immunoreactive astrocytes were dispersed throughout the entire striatum. This GFAP immunoreactivity was more pronounced in the SN. It is also important to note that GFAP immunoreactivity was elevated compared to controls 21 days following MA treatment in mice, suggesting that GFAP expression remains elevated for extended periods of time [90]. Thus, it may be possible that activation of microglia, rather than astrocytes, is associated with the acute toxic effects of MA on DA nerve terminals [55], although we cannot rule out a potential role of persistent astrocyte activation in response to acute MA-induced DA terminal toxicity.

Since microglia secrete cytotoxic agents, such as free radicals, cytokines, and chemokines, it is generally considered that microglial activation induces neurotoxicity. However, although MA treatment did not produce nigral microglial

activation (this study, [55]), we observed a significant decrease in nigral TH immunoreactivity. Surprisingly, we found that the pro-inflammatory cytokine tumor necrosis factor (TNF)α played a neuroprotective role in response to MA-induced neurotoxicity [91]. In addition, the free radical scavenger edaravone attenuated MA-induced neurotoxicity without any effect on microglial activation [92].

Thus, microglia are not the sole cause of nerve-ending damage, but serve as participants in a gradual process of glial–neuronal crosstalk that is initiated by MA-induced disruptions in presynaptic DA homeostasis [57]. More direct experiments using pharmacological and genetic manipulations of astrocyte and microglia activation are needed to determine the role of these two cell types in MA-induced DA terminal degeneration. In addition, more specific markers for the different stages of activation of both microglia and astrocytes are needed to further clarify the differences in degree of activation and activity of these two cell types following MA treatment [58].

Several investigators have demonstrated a significant correlation between a reduction in behavioral activity and the degree of striatal DA loss [93, 94]. Typically, these studies demonstrated pronounced impairments in behavioral responses that occur after a significant reduction in striatal DA content. We observed that overt impairments in both dopamine and behavioral activity induced by MA lasted for at least 14 days in PKCδ (+/+) mice. In addition, MA-induced apoptosis (i.e., TUNEL-positive cells) peaks at 24 h [26, 29, 30], while DA terminal markers (TH, DAT, and VMAT2) remain lower for 14 days after the final MA dose [26], indicating that MA-induced oxidative stress, followed by microglial activation and apoptosis, precedes DA terminal toxicity. Therefore, our results suggest that MA may be useful as a laboratory tool for modeling basal ganglia dysfunction in rodents and that PKCδ overexpression could contribute to MA-induced behavioral deficits. We assume that initial increases (mitochondria > cytosol) in reactive oxygen species potentiate PKCδ activity and that caspase-3-dependent proteolytic activation of PKCδ might mediate apoptotic death in dopaminergic cells as well as behavioral impairment.

In contrast, the MA-induced early increase in oxidative stress in PKCδ (+/+) mice returned to near control levels after 14 days. This may be attributable to positive effects of unknown neurotropic/antioxidant/anti-inflammatory substances [95, 96]. We raise the possibility that ginsenoside Re or PKCδ inhibition significantly facilitates antioxidant and neurotropic potential by positively modulating mitochondrial functions and other unknown mechanisms.

Ginsenosides are distributed throughout many parts of the ginseng plant, including the root, leaf, flower bud, and berry. Different parts of the plant contain distinct ginsenoside profiles [97], and these parts may have different pharmacological activities. The ginseng root has been mainly used as a herbal medicine, whereas other parts have been considered by-products or minor products. Earlier reports indicated that the specific ginsenoside Re is more abundant in the leaf, berry, and flower bud than in the root [12, 13, 98], reflecting possible pharmaco-economical advantages of ginsenoside Re in terms of developing natural/drug resources.

Taken together, our findings suggest that ginsenoside Re rescues MA-induced oxidative burdens (mitochondria > cytosol), mitochondrial dysfunction, pro-inflammatory changes (i.e., exacerbated activation of microglia), apoptosis, and dopaminergic degeneration via inactivation of PKCδ (Fig. 9).

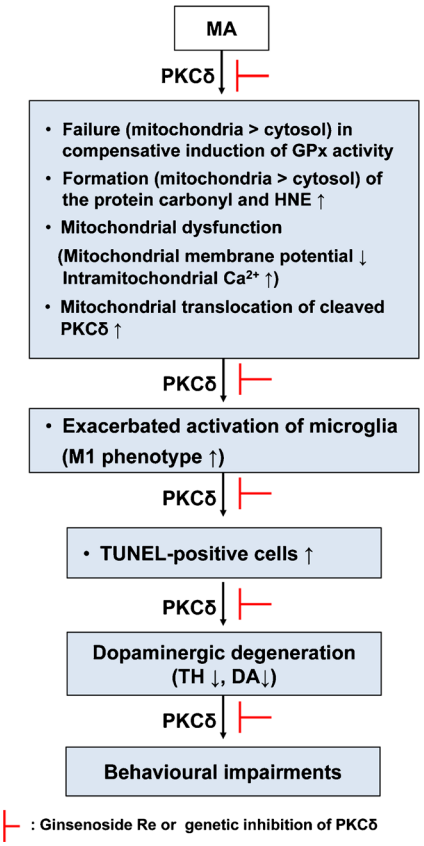

Fig. 9 A schematic depiction of ginsenoside Re-mediated protective potential in response to methamphetamine (*MA*)-induced dopaminergic neurotoxicity by PKCδ inhibition. Impairment in compensative induction of GPx activity and oxidative stress (i.e., increased protein carbonyl and HNE) induced by MA were more pronounced in mitochondria than in cytosol. These mitochondrial oxidative burdens might potentiate mitochondrial dysfunction (i.e., reduced mitochondrial membrane potential and intramitochondrial Ca^{2+}) and mitochondrial translocation of PKCδ. Mitochondrial oxidative stress and its dysfunction might facilitate pro-inflammatory changes (i.e., exacerbated activation of microglia; M1 phenotype). These changes might be essential for apoptotic cellular degeneration followed by dopaminergic degeneration. The dopaminergic degeneration may be a prerequisite for behavioral impairments. Ginsenoside Re inhibited neurotoxic signaling induced by MA by inhibiting PKCδ. Importantly, ginsenoside Re did not significantly affect neuroprotective activity mediated by genetic inhibition of PKCδ with PKCδ antisense oligonucleosides or in PKCδ-knockout (−/−) mice. Therefore, PKCδ is a critical target for dopaminergic neuroprotection mediated by ginsenoside Re

The promising efficacy of ginsenoside Re in response to MA insult could be helpful for developing medicinal preparations for PD-like conditions, although more evidence should be gathered.

Acknowledgments This study was supported by a grant (no. 110113-3) from the Korea Institute of Planning and Evaluation for Technology in Food, Agriculture, Forestry, and Fisheries (IPET), Republic of Korea. Thuy-Ty Lan Nguyen was supported by BK21 PLUS project. The English in this document has been checked by at least two professional editors, both native speakers of English. For a certificate, please see: http://www.textcheck.com/certificate/ECwpMn and http://www.textcheck.com/certificate/01ZHRL.

Conflict of Interest The authors declare that they have no conflict of interest.

References

1. Fitzmaurice PS, Tong J, Yazdanpanah M, Liu PP, Kalasinsky KS, Kish SJ (2006) Levels of 4-hydroxynonenal and malondialdehyde are increased in brain of human chronic users of methamphetamine. J Pharmacol Exp Ther 319:703–709
2. Guilarte TR (2001) Is methamphetamine abuse a risk factor in parkinsonism? Neurotoxicology 22:725–731
3. Kita T, Wagner GC, Nakashima T (2003) Current research on methamphetamine-induced neurotoxicity: animal models of monoamine disruption. J Pharmacol Sci 92:178–195
4. Wilson JM, Kalasinsky KS, Levey AI, Bergeron C, Reiber G, Anthony RM, Schmunk GA, Shannak K, Haycock JW, Kish SJ (1996) Striatal dopamine nerve terminal markers in human, chronic methamphetamine users. Nat Med 2:699–703
5. Wilson JM, Levey AI, Rajput A, Ang L, Guttman M, Shannak K, Niznik HB, Hornykiewicz O, Pifl C, Kish SJ (1996) Differential changes in neurochemical markers of striatal dopamine nerve terminals in idiopathic Parkinson's disease. Neurology 47:718–726
6. Zhong XH, Haycock JW, Shannak K, Robitaille Y, Fratkin J, Koeppen AH, Hornykiewicz O, Kish SJ (1995) Striatal dihydroxyphenylalanine decarboxylase and tyrosine hydroxylase protein in idiopathic Parkinson's disease and dominantly inherited olivopontocerebellar atrophy. Mov Disord 10:10–17
7. Kim HC, Jhoo WK, Shin EJ, Bing G (2000) Selenium deficiency potentiates methamphetamine-induced nigral neuronal loss; comparison with MPTP model. Brain Res 862:247–252
8. Sonsalla PK, Jochnowitz ND, Zeevalk GD, Oostveen JA, Hall ED (1996) Treatment of mice with methamphetamine produces cell loss in the substantia nigra. Brain Res 738:172–175
9. Lu JM, Yao Q, Chen C (2009) Ginseng compounds: an update on their molecular mechanisms and medical applications. Curr Vasc Pharmacol 7:293–302
10. Joo KM, Lee JH, Jeon HY, Park CW, Hong DK, Jeong HJ, Lee SJ, Lee SY, Lim KM (2010) Pharmacokinetic study of ginsenoside Re with pure ginsenoside Re and ginseng berry extracts in mouse using ultra performance liquid chromatography/mass spectrometric method. J Pharm Biomed Anal 51:278–283
11. Xie JT, Shao ZH, Hoek TLV, Chang WT, Li J, Mehendale S, Wang CZ, Hsu CW, Becker LB, Yin JJ, Yuan XS (2006) Antioxidant effects of ginsenoside Re in cardiomyocytes. Eur J Pharmacol 532:201–207
12. Ko SK, Bae HM, Cho OS, Im BO, Chung SH, Lee BY (2008) Analysis of ginsenoside composition of ginseng berry and seed. Food Sci Biotechnol 17:1379–1382
13. Ko SK, Cho OS, Bae HM, Im BO, Lee OH, Lee BY (2011) Quantitative analysis of ginsenosides composition in flower buds of various ginseng plants. J Korean Soc Appl Biol Chem 54:154–157
14. Bai CX, Sunami A, Namiki T, Sawanobori T, Furukawa T (2003) Electrophysiological effects of ginseng and ginsenoside Re in guinea pig ventricular myocytes. Eur J Pharmacol 476:35–44
15. Bai CX, Takahashi K, Masumiya H, Sawanobori T, Furukawa T (2004) Nitric oxide-dependent modulation of the delayed rectifier K^+ current and the L-type Ca^{2+} current by ginsenoside Re, an ingredient of *Panax ginseng*, in guinea-pig cardiomyocytes. Br J Pharmacol 142:567–575
16. Kim HS, Lee JH, Goo YS, Nah SY (1998) Effects of ginsenosides on Ca^{2+} channels and membrane capacitance in rat adrenal chromaffin cells. Brain Res Bull 46:245–251
17. Kim KH, Song K, Yoon SH, Shehzad O, Kim YS, Son JH (2012) Rescue of PINK1 protein null-specific mitochonsdrial complex IV deficits ginsenoside Re activation of nitric oxide signaling. J Biol Chem 287:44109–44120
18. Xu BB, Liu CQ, Gao X, Zhang WQ, Wang SW, Cao YL (2005) Possible mechanisms of the protection of ginsenoside Re against MPTP-induced apoptosis in substantia nigra of Parkinson's disease mouse model. J Asian Nat Prod Res 7:215–224
19. Nishizuka Y (1986) Studies and perspectives of protein kinase C. Science 233:305–312
20. Nishizuka Y (1992) Intracellular signaling by hydrolysis of phospholipids and activation of protein kinase C. Science 258:607–614
21. Basu A, Pal D (2010) Two faces of protein kinase Cδ: the contrasting roles of PKCδ in cell survival and cell death. Sci World J 10:2272–2284
22. Kanthasamy AG, Kitazawa M, Kanthasamy A, Anantharam V (2003) Role of proteolytic activation of PKCδ in oxidative stress-induced apoptosis. Antioxid Redox Signal 5:609–620
23. Kaul S, Kanthasamy A, Kitazawa M, Anantharam V, Kanthasamy AG (2003) Caspase-3 dependent proteolytic activation of protein kinase Cδ mediates and regulates 1-methyl-4-phenylpyridinium (MPP^+)-induced apoptotic cell death in dopaminergic cells: relevance to oxidative stress in dopaminergic degeneration. Eur J Neurosci 18:1387–1401
24. Zhang D, Kanthasamy A, Anantharam V (2011) Effects of manganese on tyrosine hydroxylase (TH) activity and TH-phosphorylation in a dopaminergic neural cell line. Toxicol Appl Pharmacol 254:65–71
25. Shin EJ, Duong CX, Nguyen TX, Bing G, Bach JH, Park DH, Nakayama K, Ali SF, Kanthasamy AG, Cadet JL, Nabeshima T, Kim HC (2011) PKCδ inhibition enhances tyrosine hydroxylase phosphorylation in mice after methamphetamine treatment. Neurochem Int 59:39–50
26. Shin EJ, Duong CX, Nguyen XKT, Li Z, Bing G, Bach JH, Park DH, Nakayama K, Ali SF, Kanthasamy AG, Cadet JL, Nabeshima T, Kim HC (2012) Role of oxidative stress in methamphetamine-induced dopaminergic toxicity mediated by protein kinase Cδ. Behav Brain Res 232:98–113
27. Shin EJ, Nabeshima T, Suh HW, Jhoo WK, Oh KW, Lim YK, Kim DS, Choi KH, Kim HC (2005) Ginsenosides attenuate methamphetamine-induced behavioral side effects in mice via activation of adenosine A2A receptors: possible involvements of the striatal reduction in AP-1 DNA binding activity and proenkephalin gene expression. Behav Brain Res 158:143–157
28. Miyamoto A, Nakayama K, Imaki H, Hirose S, Jiang Y, Abe M, Tsukiyama T, Nagahama H, Ohno S, Hatakeyama S, Nakayama KI (2002) Increased proliferation of B cells and auto-immunity in mice lacking protein kinase Cδ. Nature 416:865–869
29. Zhu JP, Xu W, Angulo JA (2006) Methamphetamine-induced cell death: selective vulnerability in neuronal subpopulations of the striatum in mice. Neuroscience 140:607–622

30. Zhu JP, Xu W, Angulo N, Angulo JA (2006) Methamphetamine-induced striatal apoptosis in the mouse brain: comparison of a binge to an acute bolus drug administration. Neurotoxicology 27:131–136
31. Bey EA, Xu B, Bhattacharjee A, Oldfield CM, Zhao X, Li Q, Subbulakshmi V, Feldman GM, Wientjes FB, Cathcart MK (2004) Protein kinase Cδ required for $p47^{phox}$ phosphorylation and translocation in activated human monocytes. J Immunol 173:5730–5738
32. Khodjakov A, Lizunova EM, Minin AA, Koonce MP, Gyoeva FK (1998) A specific light chain of kinesin associates with mitochondria in cultured cells. Mol Biol Cell 9:333–343
33. Xiong Y, Gu Q, Peterson PL, Muizelaar JP, Lee CP (1997) Mitochondrial dysfunction and calcium perturbation induced by traumatic brain injury. J Neurotrauma 14:23–34
34. Shin EJ, Jeong JH, Kim AY, Koh YH, Nah SY, Kim WK, Ko KH, Kim HJ, Wie MB, Kwon YS, Yoneda Y, Kim HC (2009) Protection against kainate neurotoxicity by ginsenosides: attenuation of convulsive behavior, mitochondrial dysfunction and oxidative stress. J Neurosci Res 87:710–722
35. Jhoo JH, Kim HC, Nabeshima T, Yamada K, Shin EJ, Jhoo WK, Kim W, Kang KS, Jo SA, Woo JI (2004) Beta-amyloid (1–42)-induced learning and memory deficits in mice: involvement of oxidative burdens in the hippocampus and cerebral cortex. Behav Brain Res 155:185–196
36. Aebi H (1984) Catalase in vitro. In: Abelon JN, Simon MI (eds) Methods in enzymology. Academic, New York, pp 121–126
37. Lawrence RA, Burk RF (1976) Glutathione peroxidase activity in selenium-deficient rat liver. Biochem Biophys Res Commun 71:952–958
38. Wang Q, Shin EJ, Nguyen XKT, Li Q, Bach JH, Bing G, Kim WK, Kim HC, Hong JS (2012) Endogenous dynorphin protects against neurotoxin-elicited nigrostriatal dopaminergic neuron damage and motor deficits in mice. J Neuroinflammation 9:124
39. West MJ (1993) New stereological methods for counting neurons. Neurobiol Aging 14:275–285
40. Shin EJ, Jeong JH, Bing G, Park ES, Chae JS, Yen TPH, Kim WK, Wie MB, Jung BD, Kim HJ, Lee SY, Kim HC (2008) Kainate-induced mitochondrial oxidative stress contributes to hippocampal degeneration in senescence-accelerated mice. Cell Signal 20: 645–658
41. Tran HY, Shin EJ, Saito K, Nguyen XK, Chung YH, Jeong JH, Bach JH, Park DH, Yamada K, Nabeshima T, Yoneda Y, Kim HC (2012) Protective potential of IL-6 against trimethyltin-induced neurotoxicity in vivo. Free Radic Biol Med 52:1159–1174
42. Oliver CN, Ahn BW, Moerman EJ, Goldstein S, Stadtman ER (1987) Age-related changes in oxidized proteins. J Biol Chem 262: 5488–5491
43. Bruce-Keller AJ, Geddes JW, Knapp PE, McFall RW, Keller JN, Holtsberg FW, Parthasarathy S, Steiner SM, Mattson MP (1999) Anti-death properties of TNF against metabolic poisoning: mitochondrial stabilization by MnSOD. J Neuroimmunol 93:53–71
44. Qu M, Zhou Z, Xu S, Chen C, Yu Z, Wang D (2011) Mortalin overexpression attenuates beta-amyloid-induced neurotoxicity in SH-SY5Y cells. Brain Res 1367:336–345
45. Matton MP, Keller JN, Begley JC (1998) Evidence for synaptic apoptosis. Exp Neurol 153:35–48
46. Xu S, Pi H, Chen Y, Zhang N, Guo P, Lu Y, He M, Xie J, Zhong M, Zhang Y, Yu Z, Zhou Z (2013) Cadmium induced Drp1-dependent mitochondrial fragmentation by disturbing calcium homeostasis in its hepatotoxicity. Cell Death Dis 4:e540
47. Nagatsu T, Oka K, Kato T (1979) Highly sensitive assay for tyrosine hydroxylase activity by high-performance liquid chromatography. J Chromatogr 163:247–252
48. Chance B, Sies H, Boveris A (1979) Hydroperoxide metabolism in mammalian organs. Physiol Rev 59:527–605
49. Xiong Y, Shie FS, Zhang J, Lee CP, Ho YS (2004) The protective role of cellular glutathione peroxidase against trauma-induced mitochondrial dysfunction in the mouse brain. J Stroke Cerebrovasc Dis 13:129–137
50. Mari M, Morales A, Colell A, Garcia-Ruiz C, Kaplowitz N, Fernadez-Checa JC (2013) Mitochondrial glutathione: features, regulation and role in disease. Biochim Biophys Acta 1830:3317–3328
51. Prohaska JR, Ganther HE (1976) Selenium and glutathione peroxidase in developing rat brain. J Neurochem 27:1379–1387
52. Liccione JJ, Maines MD (1988) Selective vulnerability of glutathione metabolism and cellular defense mechanisms in rat striatum to manganese. J Pharmacol Exp Ther 247:156–161
53. Mattson MP (2012) Parkinson's disease: don't mess with calcium. J Clin Invest 122:1195–1198
54. Kuwabara T, Imajoh-Ohmi S (2004) LPS-induced apoptosis is dependent upon mitochondrial dysfunction. Apoptosis 9:467–474
55. Thomas DM, Walker PD, Benjamins JA, Geddes TJ, Kuhn DM (2004) Methamphetamine neurotoxicity in dopamine nerve endings of striatum is associated with microglial activation. J Pharmacol Exp Ther 311:1–7
56. Thomas DM, Kuhn DM (2005) Attenuated microglial activation mrdiates tolerance to the neurotoxic effects of methamphetamine. J Neurochem 92:790–797
57. Kuhn DM, Francescutti-Verbeem DM, Thomas DM (2008) Dopamine disposition in the presynaptic process regulates the severity of methamphetamine-induced neurotoxicity. Ann NY Acad Sci 1139:118–126
58. Friend DM, Keefe KA (2013) Glial reactivity in resistance to methamphetamine-induced neurotoxicity. J Neurochem 125:566–574
59. Sroga JM, Jones TB, Kigerl KA, McGaughy VM, Popovich PG (2003) Rats and mice exhibit distinct inflammatory reactions after spinal cord injury. J Comp Neurol 462:223–240
60. Flemming JC, Norenberg MD, Ramsay DA, Dekban GA, Marcillo AE, Saenz AD, Pasquale-Styles M, Dietrich WD, Weaver LC (2006) The cellular inflammatory response in human spinal cords injury. Brain 129:3249–3269
61. Gordon S (2003) Alternative activation of macrophage. Nat Rev Immunol 3:23–35
62. Gordon S (2007) Macrophage heterogeneity and tissue lipids. J Clin Invest 117:89–93
63. Mantovani A, Sica A, Sozzani S, Allavena P, Vecchi A, Locati M (2004) The chemokine system in diverse forms of macrophage activation and polarization. Trends Immunol 25:677–686
64. Deng X, Cadet JL (2000) Methamphetamine-induced apoptosis is attenuated in the strata of copper-zinc superoxide dismutase transgenic mice. Mol Brain Res 83:121–124
65. Kuroda KO, Ornthanalai VG, Kato T, Murphy NP (2010) FosB null mutant mice show enhanced methamphetamine neurotoxicity: potential involvement of FosB in intracellular feed back signaling and astroglial function. Neuropsychopharmacology 35:641–655
66. Walsh SL, Wagner GC (1992) Motor impairments after methamphetamine-induced neurotoxicity in the rat. J Pharmacol Exp Ther 263:617–626
67. Kim HC, Shin EJ, Jang CG, Lee MK, Eun JS, Hong JT, Oh KW (2005) Pharmacological action of *Panax ginseng* on the behavioral toxicities induced by psychotropic agents. Arch Pharm Res 28:995–1001
68. Oh KW, Kim HS, Wagner GC (1997) Ginseng total saponin inhibits the dopaminergic depletions induced by methamphetamine. Planta Med 63:80–81
69. Wu CF, Liu YL, Song M, Liu W, Wang JH, Li X, Yang JY (2003) Protective effects of pseudoginsenoside-F11 on methamphetamine-induced neurotoxicity in mice. Pharmacol Biochem Behav 76: 103–109
70. Shin EJ, Koh YH, Kim AY, Nah SY, Jeong JH, Chae JS, Kim SC, Yen TPH, Yoon HJ, Kim WK, Ko KH, Kim HC (2009) Ginsenosides attenuate kainic acid-induced synaptosomal oxidative stress via

stimulation of adenosine A2A receptors in rat hippocampus. Behav Brain Res 197:239–245
71. Lopez MVN, Cuadrado MPGS, Ruiz-Poveda OMP, Del Frseno AMV, Acccame MEC (2007) Neuroprotective effect of individual ginsenosides on astrocytes primary culture. Biochim Biophys Acta 1770:1308–1316
72. Paul S, Shin HP, Kang SC (2012) Inhibition of inflammations and macrophage activated by ginsenoside-Re isolated from Korean ginseng (*Panax ginseng* C.A. Meyer). Food Chem Toxicol 50:1354–1361
73. Carter CA (2000) Protein kinase C as a drug target: implications for drug or diet prevention and treatment of cancer. Curr Drug Targets 1: 163–183
74. Goldberg M, Steinberg SF (1996) Tissue-specific developmental regulation of protein kinase C isoforms. Biochem Pharmacol 51: 1089–1093
75. Van Den Eeden SK, Tanner CM, Bernstein AL, Fross RD, Leimpeter A, Bloch DA, Nelson LM (2003) Incidence of Parkinson's disease: variation by age, gender, and race/ethnicity. Am J Epidemiol 157: 1015–1022
76. Callaghan RC, Cunningham JK, Sajeev G, Kish SJ (2010) Incidence of Parkinson's disease among hospital patients with methamphetamine-use disorders. Mov Disord 25:2333–2339
77. Callaghan RC, Cunningham JK, Sykes J, Kish SJ (2012) Increased risk of Parkinson's disease in individuals hospitalized with conditions related to the use of methamphetamine or other amphetamine-type drugs. Drug Alcohol Depend 120:35–40
78. Coyle JT, Puttfarcken P (1993) Oxidative stress, glutamate, and neurodegenerative disorders. Science 262:689–694
79. Halliwell B (1992) Reactive oxygen species and the central nervous system. J Neurochem 59:1609–1623
80. Hirata H, Ladenheim B, Rothman RB, Epstein C, Cadet JL (1995) Methamphetamine-induced serotonin neurotoxicity is mediated by superoxide radicals. Brain Res 677:345–347
81. Kim HC, Jhoo WK, Choi DY, Im DH, Shin EJ, Suh JH, Floyd RA, Bing G (1999) Protection of methamphetamine nigrostriatal toxicity by dietary selenium. Brain Res 851:76–86
82. Floyd RA, Carney JM (1992) Free radical damage to protein and DNA: mechanisms involved and relevant observations on brain undergoing oxidative stress. Ann Neurol 32:S22–S27
83. Asanuma M, Miyazaki I, Ogawa N (2003) Dopamine- or L-DOPA-induced neurotoxicity: the role of dopamine quinine formation and tyrosinase in a model of Parkinson's disease. Neurotox Res 5:165–176
84. Nicholls DG (2009) Mitochondrial calcium function and dysfunction in the central nervous system. Biochim Biopys Acta 1787:1416–1424
85. Ryu JK, Nagai A, Kim J, Lee MC, McLarnon JC, Kim SU (2003) Microglial activation and cell death induced by the mitochondrial toxin 3-nitropropionic acid: in vitro and in vivo studies. Neurobiol Dis 12:121–132
86. Hald A, Lotharius J (2005) Oxidative stress and inflammation in Parkinson's disease: is there a causal link? Exp Neurol 193:279–290
87. Sekine Y, Ouchi Y, Sugihara G, Takei N, Yoshikawa E, Nakamura K, Iwata Y, Tsuchiya KJ, Suda S, Suzuki K, Kawai M, Takebayashi K, Yamamoto S, Matsuzaki H, Ukei T, Mori N, Gold MS, Cadet JL (2008) Methamphetamine causes microglial activation in the brains of human abusers. J Neurosci 28:5756–5761
88. Kitamura O, Takeichi T, Wang EL, Tokunaga I, Ishigami A, Kubo S (2010) Microglial and astrocytic changes in the striatum of methamphetamine abusers. Leg Med 12:57–62
89. Burguillos MA, Deierborg T, Kavanagh E, Persson A, Hajji N, Garcia-Quintanilla A, Cano J, Brundin P, Englund E, Venero JL, Joseph B (2011) Caspase signaling controls microglia activation and neurotoxicity. Nature 472:319–325
90. O'Callaghan JP, Miller DB (1994) Neurotoxicity profiles of substituted amphetamines in the C57BL/6J mice. J Pharmacol Exp Ther 270:741–751
91. Nakajima A, Yamada K, Nagai T, Uchiyama T, Miyamoto Y, Mamiya T, He J, Nitta A, Mizuno M, Tran MH, Seto A, Yoshimura M, Kitaichi K, Hasegawa T, Saito K, Yamada Y, Seishima M, Sekikawa K, Kim HC, Nabeshima T (2004) Role of tumor necrosis factor-alpha in methamphetamine-induced drug dependence and neurotoxicity. J Neurosci 24:2212–2225
92. Kawasaki T, Ishihara K, Ago Y, Nakamura S, Itoh S, Baba A, Matsuda T (2006) Protective effect of the radical scavenger edaravone against methamphetamine-induced dopaminergic neurotoxicity in mouse striatum. Eur J Pharmacol 542:92–99
93. Jung BD, Shin EJ, Nguyen XK, Jin CH, Bach JH, Park SJ, Nah SY, Wie MB, Bing G, Kim HC (2010) Potentiation of methamphetamine neurotoxicity by intrastriatal lipopolysaccharide administration. Neurochem Int 56:229–244
94. Lenard LG, Beer B (1975) Relationship of brain levels of norepinephrine and dopamine to avoidance behavior in rats after intraventricular administration of 6-hydoxydopamine. Pharmacol Biochem Behav 3:895–899
95. Miyazaki I, Asanuma M, Kikkawa Y, Takeshima M, Murakami S, Miyoshi K, Sogawa N, Kita T (2011) Astrocyte-derived metallothionein protects dopaminergic neurons from dopamine quinone toxicity. Glia 59:435–451
96. Zhang W, Shin EJ, Wang T, Lee PH, Pang H, Wie MB, Kim WK, Kim SJ, Huang WH, Wang W, Zhang W, Hong JS, Kim HC (2006) Hydroxymorphinan, a metabolite of dextromethorphan, protects nigrostriatal pathway against MPTP-elicited damage both in vivo and in vitro. FASEB J 20:2496–2511
97. Attele AS, Wu JA, Yuan CS (1999) Ginseng pharmacology: multiple constituents and multiple actions. Biochem Pharmacol 58:1685–1693
98. Kim YK, Yoo DS, Xu H, Park NI, Kim HH, Choi JE, Park SU (2009) Ginsenoside content of berries and roots of three typical Korean ginseng (*Panax ginseng*) cultivars. Nat Prod Commun 4: 903–906